NEXT-GENERATION CARBON NON-MATERIALS INTERCONNECTS AND PASSIVE PHYSICS PRESENT STATE AND PROSPECTS, PERFORMANCE OPTIMIZATION, SENSING APPLICATIONS, AND SYSTEM INTEGRATION.

Rashmi Pancholi, Research Scholar, Department. of Physics, LNCT University, Bhopal, INDIA
rashmipancholi123@gmail.com
Dr Santosh Jain Professor, Department of Physics, LNCT University, Bhopal, INDIA

ABSTRACT:
Molecules may be found and identified with the use of infrared absorption spectroscopy. Unfortunately, the molecule's low infrared absorption cross-section limits its applicability, leading to low sensitivity and a poor signal-to-noise ratio. Utilizing the field-enhancing characteristics of periodic nanostructures, Surface-Enhanced Infrared Absorption (SEIRA) spectroscopy is a novel approach that amplifies the vibrational signals of trace molecules. Diverse sensing applications have been spurred by the intriguing features of SEIRA technology. First, we go over three methods for optimizing SEIRA performance in this review: improving bandwidth, enhancing sensitivity, and choosing the right material. Next, we go through the possible uses of SEIRA technology in domains like environmental monitoring and biomedicine. We have entered a new era marked by wearable technology, sensor networks, and the Internet of Things in recent years. The search for more compact and integrated infrared spectroscopy chips and systems was prompted by these new requirements. Furthermore, SEIRA has gained fresh life from the emergence of machine learning, which has elevated data analysis and smart device design. This analysis concludes with an exploration of the potential future trajectory of SEIRA technology, identifying emerging trends and opportunities.

KEYWORDS:
metamaterials, nanophotonic, plasmonic, light-matter interaction, sensor, chiral, machine learning, surface-enhanced infrared absorption, and two-dimensional material

INTRODUCTION

A valuable technique for characterizing materials is infrared spectroscopy, which provides non-destructive, label-free access to details on the species and chemical makeup of molecules. These intrinsic qualities have allowed infrared spectroscopy to find several ground-breaking uses in industries like environmental monitoring and medical. However, the use of conventional infrared spectroscopy in the field of trace molecular detection is restricted by the limited infrared absorption cross-section of molecules. The Beer-Lambert law, commonly referred to as Beer's law, provides an explanation for this restriction. The Beer-Lambert law can be expressed generally as follows:

$$A = \varepsilon cl \qquad (1)$$

where A is the absorbance, # is the molar absorptivity (also known as the molar absorptivity),
The material's concentration is denoted by c, while the length of light's journey through the substance is represented by l. It can be shown from Equation (1) that the absorbance A is proportional to the absorbing material's thickness (l) and concentration (c). Conventional spectrometers are unable to detect detectable absorbance in situations when the analyte's thickness is extremely thin or its concentration is extremely low. A fresh approach is desperately required to address this issue in order to further the advancement of infrared spectroscopy technology and increase the detection sensitivity of conventional infrared spectrometers. The aforementioned restrictions can be addressed in a number of ways, including by improving the infrared light source, creating extremely sensitive infrared detectors, and using the Surface-Enhanced Infrared Effect of absorption (SEIRA) The detection sensitivity of infrared spectrometers may be increased using brighter infrared light sources and more sensitive infrared detectors, although these upgrades are frequently more expensive. Conversely, SEIRA spectroscopy is an inexpensive and efficient way to improve the interaction between light and

matter. The idea of SEIRA was initially put out by Hartstein et al. in 1980 [4]. They showed a 20-fold improvement in the infrared vibrational signal of a monolayer molecular film by utilizing randomly distributed silver nanoparticles. They postulated that "collective electronic resonances excited by the incident light" were the source of the increase. Nowadays, the fundamental process behind this improvement is clearly recognized and linked to Surface Plasmon Polaritons (SPP), which are commonly paired with

Techniques for Attenuated Total Reflection (ATR) However, in the nearly 30 years after 1980, SEIRA's progress has been very sluggish. The delayed advancement of SEIRA can be attributed to two main issues. One may argue that the metal island film-based SEIRA enhancement is a non-resonant enhancement process. Because the plasmon resonance is not tuned to the infrared spectrum, it produces tiny enhancement factors that usually range from 101 to 102. Comparing this to Surface-Enhanced Raman Spectroscopy (SERS), which may get enhancement factors as high as 103 during the same time frame [9,10], is less striking. However, due to the constraints of micro/nanofabrication techniques, metal island films, which are created by gas-phase or electrochemical deposition processes, show significant structural differences. The SEIRA enhancement signal is extremely unstable due to the unpredictability in the metal island films' structural characteristics. The advent of metamaterials has presented novel prospects for enhancing the stability and sensitivity of SEIRA spectroscopy. A family of materials known as metamaterials is created intentionally and has subwavelength periodic features that enable any kind of manipulation of incident electromagnetic waves [16]. Negative refractive index [17], near-field enhancement Electromagnetically Induced Transparency (EIT), Electromagnetically Induced Absorption (EIA)], inverse Doppler shift effect, and inverse Cherenkov effect [24] are just a few of the remarkable physical properties they exhibit that are not present in natural materials. These remarkable physical properties provide a wealth of new application areas.

superlenses slow light], nonlinear optics], holography imaging [29], invisibility cloaking, and sensing are among the technologies that have arisen. In particular, metamaterials-based sensing research has gained a lot of attention lately. The resonant frequency may be adjusted to be in the mid-infrared region while producing intense and tightly contained electromagnetic field hotspots by adjusting the size of metamaterial nanoantennas. The sensitivity of SEIRA spectroscopy is greatly increased by these strong interactions with nearby analytes made possible by these powerful electromagnetic field hotspots [35]. As a result, metamaterials are now a great option for spectroscopic and biochemical sensing applications. Additionally, the development of micro/nanofabrication methods and customisable metamaterials has increased the unpredictability in the

changes in metal island films, providing the groundwork for a steady increase of SEIRA spectroscopy. The substantial SEIRA spectroscopy enhancement impact of plasmonic nanoantennas was originally shown by Neubrech et al. in 2008. In this study, Neubrech et al. engineered the size of the plasmonic nanoantennas artificially in order to produce Localized Surface Plasmon Resonance (LSPR) in the infrared range. The target analyte was a monolayer of octadecanethiol (ODT) molecules. When the analyte's resonance frequency matched the plasmonic resonance frequency, a significant SERIA enhancement was seen. Nevertheless, the specific nanoantennas' enhancing impact was restricted.

suggested using arrayed plasmonic nanoantennas for ultra-sensitive spectrum detection of protein monolayers in order to further enhance SEIRA performance [38]. In contrast to individual greater local field enhancements and more distinct spectrum responses can be obtained by using arrayed nanoantennas to induce collective electron resonances. According to experimental findings, the arrayed nanoantennas' absorption signal greatly outperformed that of the individual nanoantennas, perhaps reaching protein detection limits at the zeptomole level. Additionally, the arrayed nanoantennas showed better repeatability and dependability than single nanoantennas and chemically produced metal island films.

The development of SEIRA technology has advanced quickly since then. The evolution of SEIRA technology is summarized in this overview, which highlights four key trends: materials, increased bandwidth, sensitivity augmentation, and applications (Figure 1). The Internet of Things (IoT) in

recent years, New requirements for the system integration and downsizing of infrared spectroscopy chips and systems have been brought about by wearable technology and sensor networks. Thus, a key step towards the advancement of SEIRA technology is the downsizing and system integration of infrared spectroscopy. Furthermore, the emergence of Machine Learning (ML) has given SEIRA technology fresh life. More intelligent data analysis and device design may be made possible by leveraging ML. Viewpoints on potential developments in SEIRA technology development are covered in the review's last part.
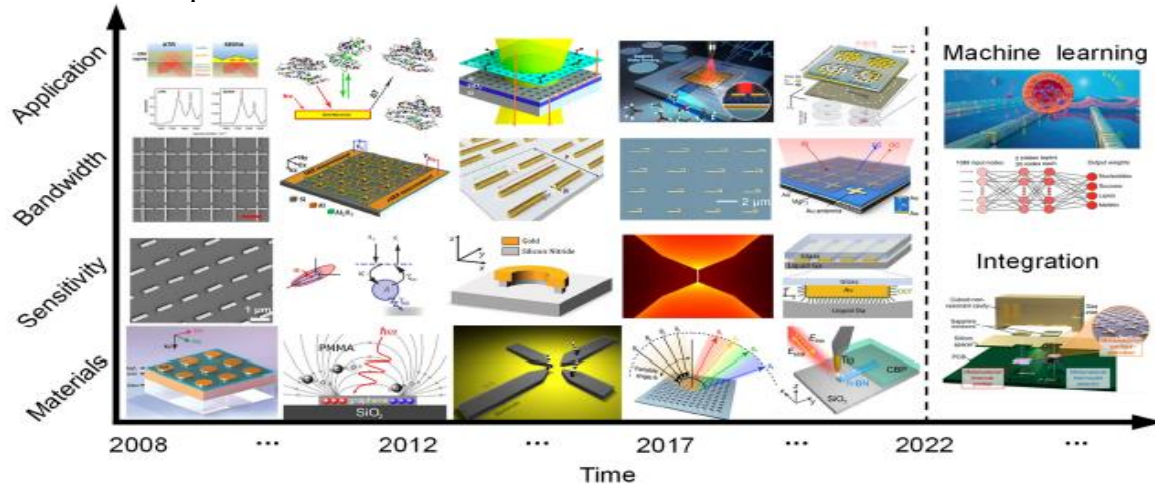

Figure 1. The SEIRA road map over the previous fifteen years, based on IR metamaterials.

3. LITERATURE REVIEWS

A. Karabchevsky et al On-chip nanophotonic devices are a class of devices capable of controlling light on a chip to realize performance advantages over ordinary building blocks of integrated photonics. These ultra-fast and low-power nanoscale optoelectronic devices are aimed at high performance computing, chemical, and biological sensing technologies, energy-efficient lighting, environmental monitoring and more. They are increasingly becoming an attractive building block in a variety of systems, which is attributed to their unique features of large evanescent field, compactness, and most importantly their ability to be configured according to the required application. This review summarizes recent advances of integrated nanophotonic devices and their demonstrated applications, including but not limited to, mid-infrared and overtone spectroscopy, all-optical processing on a chip, logic gates on a chip, and cryptography on a chip. The reviewed devices open up a new chapter in on-chip nanophotonics and enable the application of optical waveguides in a variety of optical systems, thus are aimed at accelerating the transition of nanophotonics from academia to the industry.

S. Abdollahramezani et al ; Nanophotonics has garnered intensive attention due to its unique capabilities in molding the flow of light in the subwavelength regime. Metasurfaces (MSs) and photonic integrated circuits (PICs) enable the realization of mass-producible, cost-effective, and efficient flat optical components for imaging, sensing, and communications. In order to enable nanophotonics with multipurpose functionalities, chalcogenide phase-change materials (PCMs) have been introduced as a promising platform for tunable and reconfigurable nanophotonic frameworks. Integration of non-volatile chalcogenide PCMs with unique properties such as drastic optical contrasts, fast switching speeds, and long-term stability grants substantial reconfiguration to the more conventional static nanophotonic platforms. In this review, we discuss state-of-the-art developments as well as emerging trends in tunable MSs and PICs using chalcogenide PCMs. We outline the unique material roperties, structural transformation, and thermo-optic effects of well-established classes of chalcogenide PCMs. The emerging deep learning-based approaches for the optimization of reconfigurable MSs and the analysis of light matter interactions are also discussed. The review is concluded by discussing existing challenges in the realization of adjustable nanophotonics and a perspective on the possible developments in this promising area.

A. Tripathi et al; Rare-earth-doped nanocrystals are emerging light sources that can produce tunable emissions in colours and lifetimes, which has been typically achieved in chemistry and material science. However, one important optical challenge – polarization of photoluminescence – remains largely out of control by chemistry methods. Control over photoluminescence polarization can be gained via coupling of emitters to resonant nanostructures such as optical antennas and metasurfaces. However, the resulting polarization is typically sensitive to position disorder of emitters, which is difficult to mitigate. Methods: Recently, new classes of disorder-immune optical systems have been explored within the framework of topological photonics. Here we explore disorder-robust topological arrays of Mie-resonant nanoparticles for polarization control of photoluminescence of nanocrystals. Results: We demonstrate polarized emission from rareearth- doped nanocrystals governed by photonic topological edge states supported by zigzag arrays of dielectric resonators. We verify the topological origin of polarized photoluminescence by comparing emission from nanoparticles coupled to topologically trivial and nontrivial arrays of nanoresonators.

4 OBJECTIVE OF THE STUDY

One of the materials that SEIRA uses the most frequently is metal. Metal surfaces have good optical qualities in the infrared spectrum due to their strong conductivity and Surface Plasmon Resonance (SPR) effects.

RESONATOR MATERIALS

One of the materials that SEIRA uses the most frequently is metal (Figure 2a). Metal surfaces have outstanding optical qualities in the infrared spectrum due to their strong conductivity and Surface Plasmon Resonance (SPR) phenomena. The interaction between electromagnetic waves and molecules affixed to the metal surface is improved by this phenomenon, which produces highly concentrated electric fields on the metal surface at the nanoscale. Furthermore, gold is a flexible material that may be used in biosensing due to its chemical inertness and ease of surface functionalization. It has been shown that gold-based metamaterials can also be used in other wavelength ranges, such as microwaves, terahertz, and visible light [66]. But as a valuable metal, gold has issues with affordability and sustainability.

while manufacturing SEIRA chips in bulk. Apart from gold, plasmonic resonances may also be excited by silver, copper, titanium, palladium, and aluminum. Particularly aluminum has garnered a lot of attention lately as a substitute for products made of precious metals. Low cost, plentiful reserves, compatibility with Complementary Metal-Oxide-Semiconductor (CMOS) technologies, and support for resonances throughout an incredibly broad spectral range from ultraviolet to infrared are just a few of aluminum's appealing qualities. In addition, at ambient circumstances, aluminum naturally produces a 2-4 nm thick native oxide layer. The native oxide layer allows a greater variety of covalent bonding schemes between molecules and antennas as compared to Au or Ag. Aluminum is therefore a highly rated possible SEIRA candidate material.

DIELECTRIC MATERIALS

The field of SEIRA has advanced significantly thanks to the use of metal materials. Nevertheless, low-quality (Q) factors of the resonances originate from the intrinsic Ohmic losses of metals, which also restrict their resonance linewidth [85]. Furthermore, unfavorable local heating brought on by metals' high absorbance might denaturize analytes and impede the advancement of in vivo sensing. Dielectric materials with a high refractive index and low loss have evolved as an alternative to metals in order to get over these restrictions. Dielectric resonators may sustain a variety of electric and magnetic Mie-type resonance modes that appear at different wavelengths in the scattered light spectra, as demonstrated by several studies. This capability enables fine spectrum control of the system's electric/magnetic response. Lately, dielectric material-based nanosystems have offered a platform

capable of producing ultra-sharp resonances and high-Q factors. These incredibly precise resonances provide fresh opportunities for extremely sensitive nanophotonic sensing. For instance, Ghofraniha et al. used the free-space whispering gallery mode to achieve a high-Q microlaser for low-concentration biosensing [103]. Moreover, monochromatic SEIRA sensing of certain target analytes is made possible by creating high-Q resonances that are smaller than molecule vibrational bands without the requirement for an infrared spectrometer. Currently, silicon (Si), germanium (Ge), gallium phosphate (GaP), indium phosphate (InP), and other materials are often utilized as dielectrics (Figure 2b). Due to their superior optical qualities, minimal losses, and high refractive indices, these materials are highly suitable for use in a variety of optical and nanophotonic spectroscopy. Doping also adds a new dimension to the construction of dielectric resonators. Doping offers an intriguing advantage in that resonances may be electronically tuned [106], unlike metals where resonators need to be resized for every specific spectral position. Research on dielectric materials will expand as materials science and nanotechnology progress, resulting in additional breakthroughs and chances for applications in optoelectronics and biomedicine. 2.3. Materials for Phonon Resonance Phonon resonance materials have garnered a lot of interest lately. Phonon resonance materials have the ability to relate light to phonons, which are lattice vibrations, in contrast to LSPR in metallic materials. More specifically, the heterogeneous mobility of "atoms" in the lattice can strongly couple with the electromagnetic field in ionic solids made up of positively and negatively charged "ions."

domain. Phonon-Polariton (PhP), a quasi-particle arising from the coupling of photons and optical phonons, is produced by the connection of light and lattice vibrations. PhPs from Transverse Optical (TO) to Longitudinal Optical (LO) phonon frequencies have been seen in the Reststrahlen band of polar crystals [107]. PhP modes show greater Q factors and Purcell enhancement because of the phonon scattering's strong light confinement and intrinsic low damping rates. For example, Hu et al. used near-field nanoscale FTIR spectroscopy to study the strong interaction between propagating and confined PhP modes supported by Silicon Carbide (SiC) nanorod lattices [112]. Using lattice constants to determine the development of mode hybridization, they obtained near-field spectra at local sites on the the Rabi splitting spectra of the nanorod lattice and finding prominent energy-splitting gaps. Additionally, the tight interaction between phonons and light presents intriguing opportunities for high-performance sensor systems. Using a single quartz microcylinder as an SPhP resonator, Liu et al. showed the significant link between Surface Phonon-Polaritons (SPhPs) and molecular vibrations seen in far-field studies [114]. With 4-nitrobenzyl alcohol molecules, SPhPs demonstrated unique mode splitting and anticrossing characteristics, thanks to their high-Q factors and ultra-small mode volumes. This discovery opens the door to miniaturizing mid-infrared spectroscopy and improving vibrational strong coupling sensitivity. This powerful

Hexagonal Boron Nitride (hBN), SiO2, SiC, Calcium Carbonate (CaCO3), and other polar crystal materials have also shown vibrational coupling at different infrared frequencies [119, Figure 2c].

LOW-DIMENSIONAL VAN DER WAALS MATERIALS

The high field confinement of low-dimensional van der Waals (vdW) materials offers interesting opportunities not only for phonon resonance, dielectric, and metal materials, but also for infrared sensing and nanophotonics [120]. One-dimensional (1D) carbon nanotubes and two-dimensional (2D) graphene are the two low-dimensional vdW structures in infrared sensing that have been investigated the most (Figure 2d). Through exciton effects, single-walled carbon nanotubes, for instance, have been employed for in vivo and single-molecule detection [125]. It has been demonstrated that two-dimensional vdW materials, like graphene, improve plasmonic field confinement more successfully than metal nanostructures. Moreover, graphene plasmons exhibit exceptional promise for the detection of molecule structural alterations and vibrational mode fingerprinting in dynamically adjustable infrared absorption spectroscopy. Later, Hu et al. used mid-infrared resonant graphene nanoribbons to demonstrate in situ electrical modulation of graphene plasmons over the fingerprint area [129]. At the sub-monolayer level, the highly restricted graphene plasmon polaritons obtained an extraordinarily

high detection sensitivity. The scientists were able to identify both in-plane and out-of-plane vibrational modes that are not accessible through traditional Fourier Transform Infrared (FTIR) experiments by employing the strong near-field component perpendicular to the graphene direction. Using graphene nanoribbons, they also succeeded in label-free identification of gas molecules adsorbed on the graphene surface, identifying

800 zmol/_m2 concentrations or less [130]. The limited coupling effectiveness between external light and graphene plasmon polaritons is a disadvantage, despite the fact that the high optical confinement of 2D materials is a desirable property for sensing [131]. This leads to extinction levels that are generally low, below 5%, which makes them unsuitable for use in device applications. In order to improve the plasmonic response, recent approaches have included hybrid substrates with plasmonic nanostructures, integration with photonic cavities (such as Fabry–Perot), and multilayer stacking [132]. In multilayer graphene nanoribbons, for example, Nong et al. investigated graphene plasmons [134]. They were able to significantly increase the localized graphene plasmon absorption from 3% to over 92% by integrating Fabry–Perot-type cavities. The enhanced SEIRA's performance is an order of magnitude higher than that of single-layer graphene nanostructures.

HYBRID MATERIALS

While all of the materials listed above may be utilized to create metamaterials, they each have some drawbacks. The faults of each material may be addressed and new characteristics can arise by mixing two or more of these materials to produce new structures [137]. These characteristics provide new possibilities for regulating infrared sensing and light propagation. To overcome the momentum mismatch barrier between the excitation source and the acoustic plasmons in graphene, for instance, Lee et al. created a graphene acoustic plasmonic resonator by combining graphene with ultra-flat metal strips [136]. It betters the light-matter interaction and shows nearly complete absorption (94%) of incoming mid-infrared light. Protein absorption bands at angstrom can be precisely measured using graphene acoustic plasmonics.

In SiO2, thickness and surface phonon modes. Furthermore, there has been significant interest in hybrid metal-dielectric nanostructures [138]. As an example, a hybrid metal-dielectric nanoscale antenna was created by The silicon cylinder and aluminum disk of the hybrid nanoscale antenna are separated by a SiO2 spacer. This metal-dielectric hybrid design combines many low-loss radiative channels of dielectric resonators with the high field enhancement of plasmonic metals. It has a superior optical response and a mix of favorable properties due to the connection between various materials. The hybrid metal-dielectric nanostructure may be further optimized to obtain a refractive index sensitivity of 245 nm/RIU for bulk refractive index detection. Additionally, mixing metal nanoparticles Quantum mechanical effects can also be produced using semiconductor nanoparticles. Huang and colleagues, for instance, created a plasmonic nanocavity [140] by using the interaction between gold and CdO nanocrystals. The quantum mechanical tunneling phenomenon is produced by the subnanometer gap between the CdO and gold nanocrystals. The Au-CdO nanocrystals experience a resonant blue shift as a result of the quantum mechanical tunneling phenomenon, which also enhances field and increases SEIRA signals.
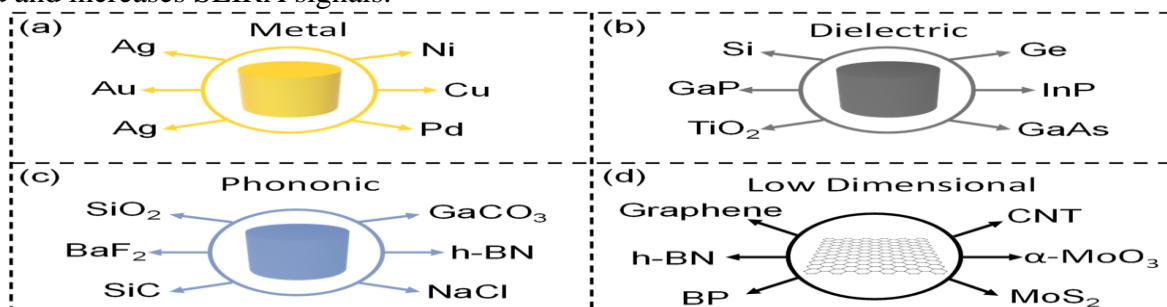

Figure 2. Choice of materials for SEIRA. (**a**) Metal materials. (b) Dielectric materials. (**c**) Phonon

resonance materials. (**d**) Low-dimensional van der Waals materials.

5. RESEARCH METHODOLOGY
SEIRA SENSITIVITY
STRUCTURAL OPTIMIZATION

Sensitivity is one of the main metrics used to assess how well EIRA is doing. The Enhancement Factor (EF) is commonly employed in assessing SEIRA's sensitivity [141].The expression of EF, which connects the increased signal intensity to the signal produced by conventional infrared methods (transmission, reflection), is as follows.

$$EF = I_{SEIRA}/I_0 / A_{SEIRA}/A_0 \qquad (2)$$

where I0 is the signal intensity without enhancement and ISEIRA is the increased signal intensity. In addition, in the SEIRA or reference measurement, ASEIRA and A0 stand for the areas (volume) covered (filled) by the molecule, respectively. Since the molecules in the antenna's hotspots are mostly responsible for the augmented SEIRA signal, ASEIRA is frequently calculated as the volume of the surface area at the tip of the antenna The near-field intensity of the metamaterial has a significant impact on SEIRA's sensitivity and detection limit. Nowadays, a typical technique for increasing near-field intensity is via decreasing the distance between neighboring nanoscale antennas. Within the nanoscale gap, the tiny gap produces a stronger field enhancement and improves the coupling between adjacent antennas. To reach a theoretical SEIRA EF of 107, for instance, Dong et al. used plasmonic junction nanoscale antennas with gaps smaller than 3 nm [49]. Refined nanoscale junction antennas including minuscule nanogaps made it possible to identify as little as 500 4-nitrophenol molecules. Yoo et al. presented a high-throughput, batch production approach based on atomic layer lithography to produce a coaxial nanohole array in order to enable large-scale manufacture of nanogaps. Using Atomic Layer Deposition (ALD) with angstrom-level thickness precision, this method produces long (up to several centimeters) and narrow (as thin as 1 nm) slits Opportunities for powerful light-matter interaction and extremely sensitive molecular sensing are presented by the ultra-small nanogaps. Research has demonstrated that an EF of 5 _ 105 was obtained for the detection of 5 nm silk protein with a nanogap size of 7 nm. Additionally, near-field intensity can be increased by making vertical nanogaps. When a metal layer is included in metamaterial absorbers, vertical nanogaps are usually used. Between the metal antennas and the metal sheet, there are substantial light confinement caused by the nanoscale vertical gaps. Molecular overlap with the near field is prevented, nonetheless, by the dielectric layer positioned between the metal sheet and the nanoscale antennas. A useful strategy to deal with this is to use microchannels as aas an alternative to the dielectric layer Le et al., for instance, presented a plasmonic-nanofluidic metamaterial made up of metal films positioned between nanofluidic channels and plasmonic resonators. The top resonator and the bottom metal mirror can move molecules more effectively and controllably thanks to this configuration, which improves the molecules' infrared absorption signal. However, it gets harder to move analyte molecules into these gaps—also known as hotspots—when microchannels get smaller and smaller until they reach the nanoscale. Particularly when the gap size is similar to the molecules' average size. This problem severely restricts the potential for future advancements in nanophotonic sensor performance. To make it easier for analytes to be transferred to the spaces between the metal layer and the antennascreated a liquid metal chip-based SEIRA sensor (Figure 3b) [55]. The sensor is composed of a metal ground plane that divides an array of metal nanobands from a nano-dielectric layer, creating a sort of tiny chip antenna array. The analyte acts as the nano-dielectric layer by physically or chemically adsorbing onto the metal nanobands. The analyte molecular layer is then covered with liquid gallium, which also functions as the nanoscale chip antenna's ground plane. It is possible to considerably improve the molecular vibrational signal associated with the analyte film because of the extremely limited and amplified electric field in the nanogap between the metal nanobands and the liquid gallium. Crucially, Such sensors are easily reusable since the liquid gallium may be withdrawn from the sensor surface after measurement. For SEIRA sensitivity, increasing the spatial overlap between molecules and

hotspots is also essential. Nevertheless, the dielectric barrier may be partially penetrated by the near-field enhancement of nanoscale antennas, reducing the likelihood of hotspots and molecules overlapping. One efficient method for creating nanopedestals is to etch the dielectric layer. For instance, Cetin et al. created polarization-insensitive mid-infrared nanoring antennas on nanopedestals and created dielectric nanopedestals using isotropic manufacturing procedures [45]. The upper antenna's hotspots are exposed to open space via the nanopedestals.

resulting in the target biomolecule and the plasmonic hotspots having the greatest possible overlap. When compared to nanoscale antennas on a substrate, SEIRA sensitivity is improved by 2.5 to 10 times because to the higher spatial overlap. Analyte solutions can also be passively captured and concentrated using dielectric nanopedestals with nanogrooves. For example, metal-insulator-metal optical resonant cavities containing nanopedestals were created by Miao et al. [152] (Figure 3c). Each dielectric nanopedestal has nanogrooves on both sides because its diameter is several hundred nanometers less than that of the top metal nanoscale antennae. The whole array of resonators is covered and the nanogrooves are penetrated by the analyte solution when it is put onto the device surface. The analyte then precipitates and deposits inside and close to the grooves as the solvent progressively evaporates. SEIRA sensitivity is further increased by the nanopedestals' passive molecular capture. The passive molecular capture made possible by nanopedestals does not work with discrete gas molecules. Gas molecules are dispersed randomly in empty space due to their weaker intermolecular interactions. Nevertheless, nanoscale antennas' poor near-field enhancement limits their capacity to detect additional gas molecules. Molecular enrichment membranes can be used to solve this problem by means of chemical or physical adsorption. For instance, ZIF-8 was utilized by Zhou et al. [156] to trap CH_4 and CO_2 inside molecular cages. This tactic increases the molecules' spatial overlap with hotspots, offering a special chance to find gas molecules. Zhou et al. then used chemical/physical synergistic adsorption to reach sub-parts-per-million (sub-PPM) detection limits for gas detection Figure 3d. Target molecules are a different strategy that is comparable to molecular enrichment membranes because they have the ability to selectively adsorb proteins, lipids, and nucleic acids in a liquid-phase environment. The collected biomolecules coincide with hotspots in the presence of target molecules, making low-concentration biomolecule identification possible. Apart from structural optimization, other techniques are available to improve sensor sensitivity. Tittl and colleagues, for instance, presented a design strategy for pixelated

All dielectric metasurfaces This approach takes use of the collective behavior of Mie resonances, which may be classified as super cavity modes driven by Bound States in Continuum (BIC) physics. In this phase, the meta surface has high-Q properties, allowing for attractive light-matter interactions. Research has revealed that the design of all-dielectric high-Q metasurfaces demonstrates considerable vibrational enhancement, enhancing sensing performance by an order of magnitude over frequently utilized metal antenna designs. Additionally, Rodrigo et al. created mid-infrared plasmonic biosensors with graphene nanoribbons [126]. Graphene's exceptional spatial confinement allows for extremely high overlap with nanoscale molecules, leading in better sensitivity in sensing their refractive indices and vibrations.

fingerprints The introduction of artificial intelligence technologies and deep learning creates new prospects for improving SEIRA sensitivity. Algorithm-driven self-iteration enables the development of unexpected, irregularly shaped photonic structures that surpass empirically specified sensitivity in sensing applications. For example, Han et al. created an optimization method that combined deep learning and genetic optimization techniques (Figure 3f) [160]. This technique employs deep learning for reverse design and optimization in order to build chiral plasmonic sensors with maximum sensitivity. Furthermore, Nanomaterials 2023, 13, 2377 9 of 38 ML can do quick analysis and automated data processing, increasing SEIRA sensitivity.
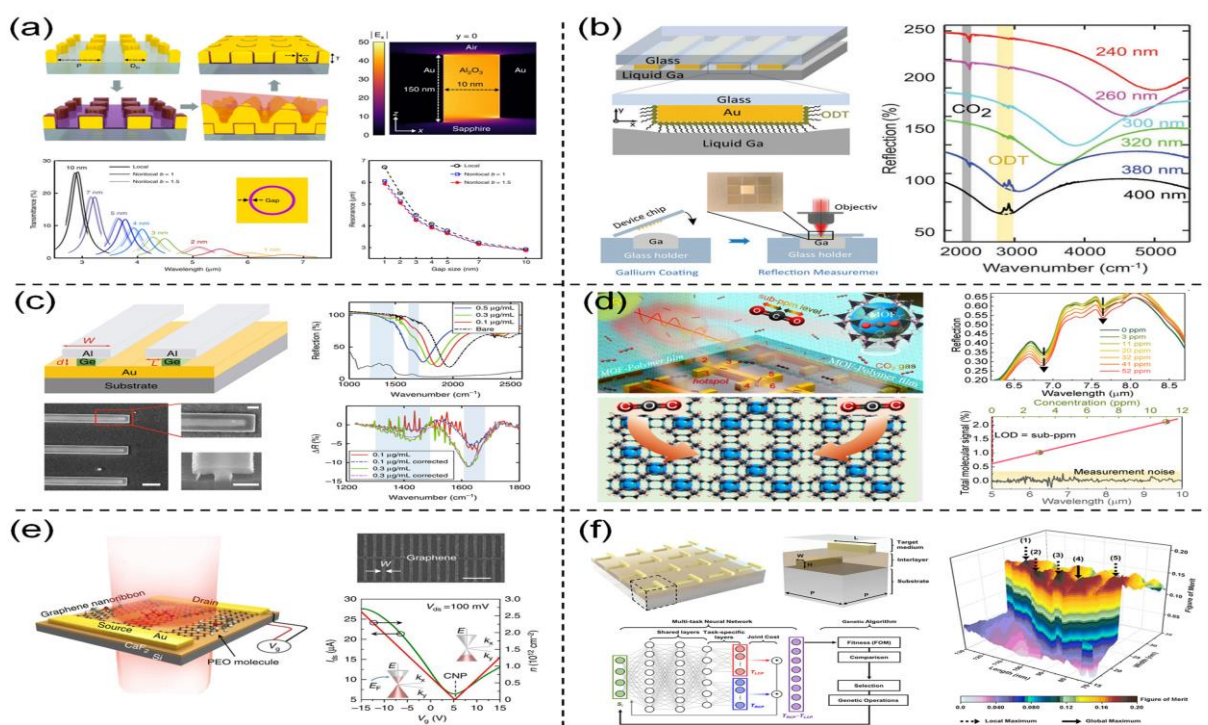
Figure 3. Plasmonic devices' sensitivity can be improved by structural optimization. (a) Extremescale nanophotonic devices having crucial gaps of just 1-2 nm. (b) Structure of liquid-gallium-based SEIRA sensors; (c) High-sensitivity nanophotonic sensors that passively trap analyte molecules in hot areas. The left picture has a scale bar of 2 _m, while the right two photos have scale bars of 600 nm. (d) MOF/polymer hybrid thin films for gas molecule enrichment. (e) Graphene plasmon enhanced molecular fingerprint sensor. (f) Structure of the forward prediction network.

.While simple structural adjustment can improve SEIRA sensitivity, it falls short of detecting infrared vibrations with nanoscale spatial precision. Infrared scattering-type Scanning Near-Field Optical Microscopy (s-SNOM) was first designed to enable nanoscale infrared spectroscopy [168]. In s-SNOM, a sharp metallic nanotip is placed near the sample and lit by incoming infrared light. The amplitude and phase of scattered light created by localized and intensified nearfield stimulation at the apex of the metallic tip provide information about the sample's refractive index and absorption coefficient [169]. Although s-SNOM enables near-field spectroscopy with nanoscale-sized

Probes, guided transport of compounds into plasmonic hotspots remains a difficult job. This difficulty is addressed using Atomic Force Microscopy-based Infrared Spectroscopy (AFM-IR) [170]. AFM-IR takes advantage of SEIRA's intrinsic near-field enhancement through the AFM tip, eliminating the necessity for targeted chemical delivery and allowing for flexible detection of molecules at any place on the substrate. Unlike s-SNOM, AFM-IR uses a pulse-wavelength-tunable infrared laser source to stimulate the sample's infrared absorption. The sample absorbs the infrared pulsed beam, resulting in heat and thermal expansion. As the As the tip approaches the sample, the thermal expansion of the sample induces a mechanical vibration in the tip with an amplitude proportional to the sample's local infrared absorption. Measure the tip amplitude while scanning the pulsed infrared laser to acquire the sample's infrared absorption spectrum. Currently, tip-enhanced infrared spectroscopy is highly sensitive and capable of detecting single molecules. detection on the nanoscale

6. CONCLUSIONS

We have described several methods for achieving SEIRA spectroscopy, ranging from metal island films with the SEIRA effect to customizable metamaterials and their current uses. This review is particularly concerned with the SEIRA effect's materials, sensitivity, bandwidth, applications, and system integration. Materials that achieve the SEIRA effect include metals, dielectrics, low-

dimensional materials, and phonon resonance materials. Each of these materials has specific features. These materials contribute to the diverse family of metamaterials, yet each has its own constraints. Combining two or more materials allows you to overcome the disadvantages of each and create new functionality. These Characteristics provide up new possibilities for managing light propagation and infrared detection. Sensitivity and bandwidth are two essential metrics that measure SEIRA's performance. Improving sensitivity allows for the detection of lower amounts of molecules, enabling a wide range of applications such as medical diagnostics and environmental monitoring. Currently, the primary techniques to enhance SEIRA sensitivity are to increase near-field intensity, increase spatial overlap between molecules and the near field, and optimize losses. Furthermore, dielectric materials capable of reaching BIC and graphene with highly restricted optical fields provide new options to improve SEIRA sensitivity. Because of the detailed structure of molecular fingerprint vibrations, increasing SEIRA bandwidth can enable access to additional vibrational information, allowing molecular retrieval. To achieve multi-band or broadband resonances,

 Several design approaches have been proposed, including fractal geometry, asymmetric structures, self-similar structures, supercells, pixelated metasurfaces, and electrically modulated metasurfaces. Loss engineering allows for the customization of metamaterials, as well as the creation of new broadband spectra. Furthermore, in recent years, there has been a lot of interest in using machine learning to inversely construct plasmonic nanostructures with high sensitivity and broadband properties. Plasmonic nanostructures bridge the length-scale gap between infrared wavelengths (micrometers) and molecular analyte sizes (nanometers), enabling novel sensing applications. Currently, sensing based on plasmonic nanostructures has covered numerous states of matter, including solids, liquids, and gases, and has found applications in varied domains such as biomedicine and environmental monitoring.

Chemistry, materials, and more. This review focuses on the use of plasmonic nanostructures in biomedicine and environmental sensing. However, most metamaterials' extensive use in sensing is hampered by their need on cumbersome spectrometers or optical systems. To address this constraint, downsizing of infrared spectroscopy has become more attractive, as it has the potential to revolutionize the industry and enable new applications in areas such as IoT and sensor networks. Extensive attempts have been made to construct small-scale spectrometers via system integration. Future optical systems are expected to be significantly downsized and integrated on a single chip. These chip-based experimental systems will enable more widespread applications in consumer technology and wearable gadgets.

7.REFERENCES

1. Swinehart, D.F. The Beer-Lambert law. J. Chem. Educ. **1962**, 39, 333–335. [CrossRef]

2. Zhou, H.; Li, D.X.; Hui, X.D.; Mu, X.J. Infrared metamaterial for surface-enhanced infrared absorption spectroscopy: Pushing the frontier of ultrasensitive on-chip sensing. Int. J. Optomechatron. **2021**, 15, 97–119. [CrossRef]

3. Neubrech, F.; Huck, C.; Weber, K.; Pucci, A.; Giessen, H. Surface-Enhanced Infrared Spectroscopy Using Resonant Nanoantennas. Chem. Rev. **2017**, 117, 5110–5145. [CrossRef] [PubMed]

4. Hartstein, A.; Kirtley, J.R.; Tsang, J.C. Enhancement of the Infrared-Absorption from Molecular Monolayers with Thin Metal Overlayers. Phys. Rev. Lett. **1980**, 45, 201–204. [CrossRef]

5. Welford, K. Surface-Plasmon Polaritons and Their Uses. Opt. Quantum Electron. **1991**, 23, 1–27. [CrossRef]

6. Noginov, M.A.; Zhu, G.; Mayy, M.; Ritzo, B.A.; Noginova, N.; Podolskiy, V.A. Stimulated emission of surface plasmon polaritons. Phys. Rev. Lett. **2008**, 101, 226806. [CrossRef]

7. Aroca, R.F.; Ross, D.J.; Domingo, C. Surface-enhanced infrared spectroscopy. Appl. Spectrosc. **2004**, 58, 324A–338A. [CrossRef]

8. Ataka, K.; Heberle, J. Biochemical applications of surface-enhanced infrared absorption spectroscopy. Anal. Bioanal. Chem. **2007**, 388, 47–54. [CrossRef]

9. Kneipp, K.;Wang, Y.; Kneipp, H.; Perelman, L.T.; Itzkan, I.; Dasari, R.; Feld,M.S. Single molecule detection using surface-enhanced Raman scattering (SERS). Phys. Rev. Lett. **1997**, 78, 1667–1670. [CrossRef]

10. Nie, S.M.; Emery, S.R. Probing single molecules and single nanoparticles by surface-enhanced Raman scattering. Science **1997**, 275, 1102–1106. [CrossRef]

11. Zheludev, N.I. The Road Ahead for Metamaterials. Science **2010**, 328, 582–583. [CrossRef] [PubMed]

12. Halas, N.J.; Lal, S.; Chang, W.S.; Link, S.; Nordlander, P. Plasmons in Strongly Coupled Metallic Nanostructures. Chem. Rev. **2011**, 111, 3913–3961. [CrossRef]

13. Brolo, A.G. Plasmonics for future biosensors. Nat. Photonics **2012**, 6, 709–713. rossRef]

14. Yang, X.X.; Sun, Z.P.; Low, T.; Hu, H.; Guo, X.D.; de Abajo, F.J.G.; Avouris, P.; Dai, Q. Nanomaterial-Based Plasmon-Enhanced Infrared Spectroscopy. Adv. Mater. **2018**, 30, 704896. [CrossRef]

15. Yang, K.; Yao, X.; Liu, B.W.; Ren, B. Metallic Plasmonic Array Structures: Principles, Fabrications, Properties, and Applications. Adv. Mater. **2021**, 33, 2007988. [CrossRef]

16. Schuller, J.A.; Barnard, E.S.; Cai, W.; Jun, Y.C.; White, J.S.; Brongersma, M.L. Plasmonics for extreme light concentration and manipulation. Nat. Mater. **2010**, 9, 193–204. [CrossRef] [PubMed]

17. Smith, D.R.; Pendry, J.B.;Wiltshire, M.C.K. Metamaterials and negative refractive index. Science **2004**, 305, 788–792. [CrossRef]

18. Schnell, M.; Garcia-Etxarri, A.; Huber, A.J.; Crozier, K.; Aizpurua, J.; Hillenbrand, R. Controlling the near-field oscillations of loaded plasmonic nanoantennas. Nat. Photonics **2009**, 3, 287–291. [CrossRef]

19. Liu, N.; Langguth, L.; Weiss, T.; Kastel, J.; Fleischhauer, M.; Pfau, T.; Giessen, H. Plasmonic analogue of electromagnetically

induced transparency at the Drude damping limit. Nat. Mater. **2009**, 8, 758–762. [CrossRef]

20. Taubert, R.; Hentschel, M.; Kastel, J.; Giessen, H. Classical Analog of electromagnetically Induced Absorption in Plasmonics. Nano Lett. **2012**, 12, 1367–1371. [CrossRef]

21. Floess, D.; Hentschel, M.; Weiss, T.; Habermeier, H.U.; Jiao, J.; Tikhodeev, S.G.; Giessen, H. Plasmonic Analog of Electromagnetically Induced Absorption Leads to Giant Thin Film Faraday Rotation of 14 degrees. Phys. Rev. X **2017**, 7, 021048.

22. Chen, J.B.; Wang, Y.; Jia, B.H.; Geng, T.; Li, X.P.; Feng, L.; Qian, W.; Liang, B.M.; Zhang, X.X.; Gu, M.; et al. Observation of the inverse Doppler effect in negative-index materials at optical frequencies. Nat. Photonics **2011**, 5, 239–242. [CrossRef]

23. Seddon, N.; Bearpark, T. Observation of the inverse Doppler effect. Science **2003**, 302, 1537–1540. [CrossRef]

24. Parazzoli, C.G.; Greegor, R.B.; Li, K.; Koltenbah, B.E.C.; Tanielian, M. Experimental verification and simulation of negative index of refraction using Snell's law. Phys. Rev. Lett. **2003**, 90, 107401. [CrossRef]

25. Wang, S.M.; Wu, P.C.; Su, V.C.; Lai, Y.C.; Chen, M.K.; Kuo, H.Y.; Chen, B.H.; Chen, Y.H.; Huang, T.T.; Wang, J.H.; et al. A broadband achromatic metalens in the visible. Nat. Nanotechnol. **2018**, 13, 227–232. [CrossRef] [PubMed]

26. Fan, Z.B.; Qiu, H.Y.; Zhang, H.L.; Pang, X.N.; Zhou, L.D.; Liu, L.; Ren, H.; Wang, Q.H.; Dong, J.W. A broadband achromatic metalens array for integral imaging in the visible. Light Sci. Appl. **2019**, 8, 67. [CrossRef]

27. Baba, T. Slow light in photonic crystals. Nat. Photonics **2008**, 2, 465–473. [CrossRef]

28. Li, G.; Zhang, S.; Zentgraf, T. Nonlinear photonic metasurfaces. Nat. Rev. Mater. **2017**, 2, 17010. [CrossRef]

29. Almeida, E.; Bitton, O.; Prior, Y. Nonlinear metamaterials for holography. Nat. Commun. **2016**, 7, 12533. [CrossRef]

30. Cai, W.S.; Chettiar, U.K.; Kildishev, A.V.; Shalaev, V.M. Optical cloaking with metamaterials. Nat. Photonics **2007**, 1, 224–227. [CrossRef]

31. Sreekanth, K.V.; Alapan, Y.; ElKabbash, M.; Ilker, E.; Hinczewski, M.; Gurkan, U.A.; De Luca, A.; Strangi, G. Extreme sensitivity biosensing platform based on hyperbolic metamaterials. Nat. Mater. **2016**, 15, 621–628. [CrossRef] [PubMed]

32. Wang, W.; Ramezani, M.; Vakevainen, A.I.; Torma, P.; Rivas, J.G.; Odom, T.W. The rich photonic world of plasmonic nanoparticle arrays. Mater. Today **2018**, 21, 303–314. [CrossRef]

33. Altug, H.; Oh, S.H.; Maier, S.A.; Homola, J. Advances and applications of nanophotonic biosensors. Nat. Nanotechnol. **2022**, 17, 5–16. [CrossRef] [PubMed]

34. Leitis, A.; Tseng, M.L.; John-Herpin, A.; Kivshar, Y.S.; Altug, H. Wafer-Scale Functional Metasurfaces for Mid-Infrared Photonics and Biosensing. Adv. Mater. **2021**, 33, 2102232. [CrossRef] [PubMed]

35. Tittl, A.; John-Herpin, A.; Leitis, A.; Arvelo, E.R.; Altug, H. Metasurface-Based Molecular Biosensing Aided by Artificial Intelligence. Angew. Chem. Int. Ed. **2019**, 58, 14810–14822. [CrossRef] [PubMed]

36. Oh, S.H.; Altug, H. Performance metrics and enabling technologies for nanoplasmonic biosensors. Nat. Commun. **2018**, 9, 5263. [CrossRef]

37. Neubrech, F.; Pucci, A.; Cornelius, T.W.; Karim, S.; Garcia-Etxarri, A.; Aizpurua, J. Resonant Plasmonic and Vibrational Coupling in a Tailored Nanoantenna for Infrared Detection. Phys. Rev. Lett. **2008**, 101, 157403. [CrossRef] [PubMed]

38. Adato, R.; Yanik, A.A.; Amsden, J.J.; Kaplan, D.L.; Omenetto, F.G.; Hong, M.K.; Erramilli, S.; Altug, H. Ultra-sensitive vibrational spectroscopy of protein monolayers with plasmonic nanoantenna arrays. Proc. Natl. Acad. Sci. USA **2009**, 106, 19227–19232.
[CrossRef] [PubMed]

39. Liu, N.; Mesch, M.; Weiss, T.; Hentschel, M.; Giessen, H. Infrared Perfect Absorber and Its Application as Plasmonic Sensor. Nano Lett. **2010**, 10, 2342–2348. [CrossRef] [PubMed]

40. Chen, K.; Adato, R.; Altug, H. Dual-band perfect absorber for multispectral plasmon-enhanced infrared spectroscopy. ACS Nano **2012**, 6, 7998–8006. [CrossRef]

41. Jiang, X.; Zaitseva, E.; Schmidt, M.; Siebert, F.; Engelhard, M.; Schlesinger, R.; Ataka, K.; Vogel, R.; Heberle, J. Resolving voltage-dependent structural changes of a membrane photoreceptor by surface-enhanced IR difference spectroscopy. Proc. Natl. Acad. Sci. USA **2008**, 105, 12113–12117. [CrossRef] [PubMed]

42. Li, Y.; Yan, H.; Farmer, D.B.; Meng, X.; Zhu,W.; Osgood, R.M.; Heinz, T.F.; Avouris, P. Graphene Plasmon Enhanced Vibrational Sensing of Surface-Adsorbed Layers. Nano Lett. **2014**, 14, 1573–1577. [CrossRef] [PubMed]

43. Adato, R.; Artar, A.; Erramilli, S.; Altug, H. Engineered absorption enhancement and induced transparency in coupled molecular and plasmonic resonator systems. Nano Lett. **2013**, 13, 2584–2591. [CrossRef]

44. Cerjan, B.; Yang, X.; Nordlander, P.; Halas, N.J. Asymmetric Aluminum Antennas for Self-Calibrating Surface Enhanced Infrared Absorption Spectroscopy. ACS Photonics **2016**, 3, 354–360. [CrossRef]

45. Cetin, A.E.; Etezadi, D.; Altug, H. Accessible Nearfields by Nanoantennas on Nanopedestals for Ultrasensitive Vibrational Spectroscopy. Adv. Opt. Mater. **2014**, 2, 866–872. [CrossRef]

46. Pitchappa, P.; Ho, C.P.; Dhakar, L.; Lee, C. Microelectromechanically reconfigurable interpixelated metamaterial for independent tuning of multiple resonances at terahertz spectral region. Optica **2015**, 2, 571. [CrossRef]

47. Rodrigo, D.; Tittl, A.; Ait-Bouziad, N.; John-Herpin, A.; Limaj, O.; Kelly, C.; Yoo, D.;Wittenberg, N.J.; Oh, S.H.; Lashuel, H.A.; et al. Resolving molecule-specific information in dynamic lipid membrane processes with multi-resonant infrared metasurfaces. Nat.
Commun. **2018**, 9, 2160. [CrossRef]

48. Mahmoudi, M.; Lohse, S.E.; Murphy, C.J.; Fathizadeh, A.; Montazeri, A.; Suslick, K.S. Variation of protein corona composition of gold nanoparticles following plasmonic heating. Nano Lett. **2014**, 14, 6–12. [CrossRef]

49. Dong, L.; Yang, X.; Zhang, C.; Cerjan, B.; Zhou, L.; Tseng, M.L.; Zhang, Y.; Alabastri, A.; Nordlander, P.; Halas, N.J. Nanogapped Au Antennas for Ultrasensitive Surface-Enhanced Infrared Absorption Spectroscopy. Nano Lett. **2017**, 17, 5768–5774. [CrossRef]

50. Chang, Y.; Hasan, D.; Dong, B.; Wei, J.; Ma, Y.; Zhou, G.; Ang, K.W.; Lee, C. All-Dielectric Surface-Enhanced Infrared Absorption- Based Gas Sensor Using Guided Resonance. ACS Appl. Mater. Interfaces **2018**, 10, 38272–38279. [CrossRef]

51. Leitis, A.; Tittl, A.; Liu, M.; Lee, B.H.; Gu, M.B.; Kivshar, Y.S.; Altug, H. Angle-multiplexed all-dielectric metasurfaces for broadband molecular fingerprint retrieval. Sci. Adv. **2019**, 5, eaaw2871. [CrossRef] [PubMed]

52. Ren, Z.; Zhang, Z.; Wei, J.; Dong, B.; Lee, C. Wavelength-multiplexed hook nanoantennas for machine learning enabled mid-infrared spectroscopy. Nat. Commun. **2022**, 13, 3859. [CrossRef] [PubMed]

53. Xu, J.; Ren, Z.; Dong, B.; Liu, X.; Wang, C.; Tian, Y.; Lee, C. Nanometer-Scale Heterogeneous Interfacial Sapphire Wafer Bonding for Enabling Plasmonic-Enhanced Nanofluidic Mid-Infrared Spectroscopy. ACS Nano **2020**, 14, 12159–12172. [CrossRef] [PubMed]

54. Li, D.; Zhou, H.; Chen, Z.; Ren, Z.; Xu, C.; He, X.; Liu, T.; Chen, X.; Huang, H.; Lee, C.; et al. Ultrasensitive Molecular Fingerprint Retrieval Using Strongly Detuned Overcoupled Plasmonic Nanoantennas. Adv. Mater. **2023**, 35, e2301787. [CrossRef]

55. Miao, X.L.; Luk, T.S.; Liu, P.Q. Liquid-Metal-Based Nanophotonic Structures for High-Performance SEIRA Sensing. Adv. Mater. **2022**, 34, e2107950. [CrossRef]

56. Dolado, I.; Maciel-Escudero, C.; Nikulina, E.; Modin, E.; Calavalle, F.; Chen, S.; Bylinkin, A.; Alfaro-Mozaz, F.J.; Li, J.; Edgar, J.H.; et al. Remote near-field spectroscopy of vibrational strong coupling between organic molecules and phononic nanoresonators.
Nat. Commun. **2022**, 13, 6850. [CrossRef]

57. Lochbaum, A.; Dorodnyy, A.; Koch, U.; Koepfli, S.M.; Volk, S.; Fedoryshyn, Y.; Wood, V.; Leuthold, J. Compact Mid-Infrared Gas Sensing Enabled by an All-Metamaterial Design. Nano Lett. **2020**, 20, 4169–4176. [CrossRef]

58. Ansaryan, S.; Liu, Y.C.; Li, X.; Economou, A.M.; Eberhardt, C.S.; Jandus, C.; Altug, H. High-throughput spatiotemporal monitoring of single-cell secretions via plasmonic microwell arrays. Nat. Biomed. Eng. **2023**, 7, 943–958. [CrossRef]

59. Zheng, J.; Cheng, X.; Zhang, H.; Bai, X.; Ai, R.; Shao, L.; Wang, J. Gold Nanorods: The Most Versatile Plasmonic Nanoparticles. Chem. Rev. **2021**, 121, 13342–13453. [CrossRef]

60. John-Herpin, A. Metasurface-Enhanced Infrared Spectroscopy: An Abundance of Materials and Functionalities. Adv. Mater. **2022**, e2110163. [CrossRef]

61. Adato, R.; Altug, H. In-situ ultra-sensitive infrared absorption spectroscopy of biomolecule interactions in real time with plasmonic nanoantennas. Nat. Commun. **2013**, 4, 2154. [CrossRef]

62. Hui, X.; Yang, C.; Li, D.; He, X.; Huang, H.; Zhou, H.; Chen, M.; Lee, C.; Mu, X. Infrared Plasmonic Biosensor with Tetrahedral DNA Nanostructure as Carriers for Label-Free and Ultrasensitive Detection of miR-155. Adv. Sci. **2021**, 8, e2100583. [CrossRef] [PubMed]

63. John-Herpin, A.; Kavungal, D.; von Mucke, L.; Altug, H. Infrared Metasurface Augmented by Deep Learning for Monitoring Dynamics between All Major Classes of Biomolecules. Adv. Mater. **2021**, 33, e2006054. [CrossRef] [PubMed]

64. Kim, J.Y.; Kim, H.; Kim, B.H.; Chang, T.; Lim, J.; Jin, H.M.; Mun, J.H.; Choi, Y.J.; Chung, K.; Shin, J.; et al. Highly tunable refractive index visible-light metasurface from block copolymer self-assembly. Nat. Commun. **2016**, 7, 12911. [CrossRef] [PubMed]

65. Zhou, H.; Yang, C.; Hu, D.; Li, D.; Hui, X.; Zhang, F.; Chen, M.; Mu, X. Terahertz biosensing based on bi-layer metamaterial absorbers toward ultra-high sensitivity and simple fabrication. Appl. Phys. Lett. **2019**, 115, 143507. [CrossRef]

66. Zhou, H.; Hu, D.; Yang, C.; Chen, C.; Ji, J.; Chen, M.; Chen, Y.; Yang, Y.; Mu, X. Multi-Band Sensing for Dielectric Property of Chemicals Using Metamaterial Integrated Microfluidic Sensor. Sci. Rep. **2018**, 8, 14801. [CrossRef]

67. Liu, X.Y.; Liu,W.D.; Yang, B. Deep-elliptical-silver-nanowell arrays (d-EAgNWAs) fabricated by stretchable imprinting combining colloidal lithography: A highly sensitive plasmonic sensing platform. Nano Res. **2019**, 12, 845–853. [CrossRef]

68. Zhuo, X.L.; Yip, H.K.; Ruan, Q.F.; Zhang, T.K.; Zhu, X.Z.; Wang, J.F.; Lin, H.Q.; Xu, J.B.; Yang, Z. Broadside Nanoantennas Made of Single Silver Nanorods. ACS Nano **2018**, 12, 1720–1731. [CrossRef]

69. Li, N.N.; Yin, H.; Zhuo, X.L.; Yang, B.C.; Zhu, X.M.; Wang, J.F. Infrared-Responsive Colloidal Silver Nanorods for Surface- Enhanced Infrared Absorption. Adv. Opt. Mater. **2018**, 6, 1800436. [CrossRef]

70. Jin, D.F.; Hu, Q.; Neuhauser, D.; von Cube, F.; Yang, Y.Y.; Sachan, R.; Luk, T.S.; Bell, D.C.; Fang, N.X. Quantum-Spillover-Enhanced Surface-Plasmonic Absorption at the Interface of Silver and High-Index Dielectrics. Phys. Rev. Lett. **2015**, 115, 193901. [CrossRef]

71. Bohme, A.; Sterl, F.; Kath, E.; Ubl, M.; Manninen, V.; Giessen, H. Electrochemistry on Inverse Copper Nanoantennas: Active Plasmonic Devices with Extraordinarily Large Resonance Shift. ACS Photonics **2019**, 6, 1863–1868. [CrossRef]

72. Tzschoppe, M.; Huck, C.; Vogt, J.; Neubrech, F.; Pucci, A. Impact of Metal-Optical Properties on Surface-Enhanced Infrared Absorption. J. Phys. Chem. C **2018**, 122, 15678–15687. [CrossRef]

73. Liu, Z.; Liu, G.; Liu, X.; Wang, Y.; Fu, G. Titanium resonators based ultra-broadband perfect light absorber. Opt. Mater. **2018**, 83, 118–123. [CrossRef]

74. Zhou, Y.; Qin, Z.; Liang, Z.; Meng, D.; Xu, H.; Smith, D.R.; Liu, Y. Ultra-broadband metamaterial absorbers from long to very long infrared regime. Light Sci. Appl. **2021**, 10, 138. [CrossRef] [PubMed]

75. Herkert, E.; Sterl, F.; Strohfeldt, N.;Walter, R.; Giessen, H. Low-Cost Hydrogen Sensor in the ppm Range with Purely Optical Readout. ACS Sens. **2020**, 5, 978–983. [CrossRef]

76. Duan, X.Y.; Kamin, S.; Sterl, F.; Giessen, H.; Liu, N. Hydrogen-Regulated Chiral Nanoplasmonics. Nano Lett. **2016**, 16, 1462–1466. [CrossRef]

77. Tittl, A.; Mai, P.; Taubert, R.; Dregely, D.; Liu, N.; Giessen, H. Palladium-Based Plasmonic Perfect Absorber in the Visible Wavelength Range and Its Application to Hydrogen Sensing. Nano Lett. **2011**, 11, 4366–4369. [CrossRef]

78. Liu, N.; Tang, M.L.; Hentschel, M.; Giessen, H.; Alivisatos, A.P. Nanoantenna-enhanced gas sensing in a single tailored nanofocus. Nat. Mater. **2011**, 10, 631–636. [CrossRef]

79. Najem, M.; Carcenac, F.; Taliercio, T.; Gonzalez-Posada, F. Aluminum Bowties for Plasmonic-Enhanced Infrared Sensing. Adv. Opt. Mater. **2022**, 10, 2201025. [CrossRef]

80. Su, M.-N.; Dongare, P.D.; Chakraborty, D.; Zhang, Y.; Yi, C.;Wen, F.; Chang,W.-S.; Nordlander, P.; Sader, J.E.; Halas, N.J.; et al. Optomechanics of Single Aluminum Nanodisks. Nano Lett. **2017**, 17, 2575–2583. [CrossRef]

81. Zhou, L.; Zhang, C.; McClain, M.J.; Manavacas, A.; Krauter, C.M.; Tian, S.; Berg, F.; Everitt, H.O.; Carter, E.A.; Nordlander, P.; et al. Aluminum Nanocrystals as a Plasmonic Photocatalyst for Hydrogen Dissociation. Nano Lett. **2016**, 16, 1478–1484. [CrossRef]

82. Chen, K.; Thang Duy, D.; Ishii, S.; Aono, M.; Nagao, T. Infrared Aluminum Metamaterial Perfect Absorbers for Plasmon-Enhanced Infrared Spectroscopy. Adv. Funct. Mater. **2015**, 25, 6637–6643. [CrossRef]

83. Martin, J.; Plain, J. Fabrication of aluminium nanostructures for plasmonics. J. Phys. D-Appl. Phys. **2015**, 48, 184002. [CrossRef]

84. Canalejas-Tejero, V.; Herranz, S.; Bellingham, A.; Moreno-Bondi, M.C.; Barrios, C.A. Passivated aluminum nanohole arrays for label-free biosensing applications. ACS Appl. Mater. Interfaces **2014**, 6, 1005–1010. [CrossRef]

85. Tittl, A.; Leitis, A.; Liu, M.; Yesilkoy, F.; Choi, D.Y.; Neshev, D.N.; Kivshar, Y.S.; Altug, H. Imaging-based molecular barcoding with pixelated dielectric metasurfaces. Science **2018**, 360, 1105–1109. [CrossRef] [PubMed]

86. Bontempi, N.; Chong, K.E.; Orton, H.W.; Staude, I.; Choi, D.-Y.; Alessandri, I.; Kivshar, Y.S.; Neshev, D.N. Highly sensitive biosensors based on all-dielectric nanoresonators. Nanoscale **2017**, 9, 4972–4980. [CrossRef]

87. Hogan, N.J.; Urban, A.S.; Ayala-Orozco, C.; Pimpinelli, A.; Nordlander, P.; Halas, N.J. Nanoparticles heat through light localization. Nano Lett. **2014**, 14, 4640–4645. [CrossRef]

88. Kuznetsov, A.I.; Miroshnichenko, A.E.; Brongersma, M.L.; Kivshar, Y.S.; Luk'yanchuk, B. Optically resonant dielectric nanostructures. Science **2016**, 354, aag2472. [CrossRef]

89. Decker,M.; Staude, I. Resonant dielectric nanostructures: A low-loss platform for functional nanophotonics. J. Opt. **2016**, 18, 103001. [CrossRef]

90. Zheludev, N.I.; Kivshar, Y.S. From metamaterials to metadevices. Nat. Mater. **2012**, 11, 917–924. [CrossRef]

91. Attiaoui, A.; Daligou, G.; Assali, S.; Skibitzki, O.; Schroeder, T.; Moutanabbir, O. Polarization-Tuned Fano Resonances in All-Dielectric Short-Wave Infrared Metasurface. Adv. Mater. **2023**, 35, e2300595. [CrossRef] [PubMed]

92. Jahani, S.; Jacob, Z. All-dielectric metamaterials. Nat. Nanotechnol. **2016**, 11, 23–36. [CrossRef]

93. Krasnok, A.; Caldarola, M.; Bonod, N.; Alu, A. Spectroscopy and Biosensing with Optically Resonant Dielectric Nanostructures. Adv. Opt. Mater. **2018**, 6, 1701094. [CrossRef]

94. Koshelev, K.; Kivshar, Y. Dielectric Resonant Metaphotonics. ACS Photonics **2021**, 8, 102–112. [CrossRef]

95. Melik-Gaykazyan, E.; Koshelev, K.; Choi, J.-H.; Kruk, S.S.; Bogdanov, A.; Park, H.-G.; Kivshar, Y. From Fano to Quasi-BIC Resonances in Individual Dielectric Nanoantennas. Nano Lett. **2021**, 21, 1765–1771. [CrossRef] [PubMed]

96. Tseng, M.L.; Jahani, A.; Leitis, A.; Altug, H. Dielectric Metasurfaces Enabling Advanced Optical Biosensors. ACS Photonics **2021**, 8, 47–60. [CrossRef]

97. Wang, J.; Kuhne, J.; Karamanos, T.; Rockstuhl, C.; Maier, S.A.; Tittl, A. All-Dielectric Crescent Metasurface Sensor Driven by Bound States in the Continuum. Adv. Funct. Mater. **2021**, 31, 2104652. [CrossRef]

98. Moretti, G.Q.; Tittl, A.; Cortés, E.; Maier, S.A.; Bragas, A.V.; Grinblat, G. Introducing a Symmetry-Breaking Coupler into a Dielectric Metasurface Enables Robust High-Q Quasi-BICs. Adv. Photonics Res. **2022**, 3, 2200111. [CrossRef]

99. Koshelev, K.; Kruk, S.; Melik-Gaykazyan, E.; Choi, J.H.; Bogdanov, A.; Park, H.G.; Kivshar, Y. Subwavelength dielectric resonators for nonlinear nanophotonics. Science **2020**, 367, 288–292. [CrossRef]

100. Conteduca, D.; Barth, I.; Pitruzzello, G.; Reardon, C.P.; Martins, E.R.; Krauss, T.F. Dielectric nanohole array metasurface for high-resolution near-field sensing and imaging. Nat. Commun. **2021**, 12, 3293. [CrossRef]

101. Barth, I.; Conteduca, D.; Reardon, C.; Johnson, S.; Krauss, T.F. Common-path interferometric label-free protein sensing with resonant dielectric nanostructures. Light Sci. Appl. **2020**, 9, 96. [CrossRef] [PubMed]

102. Yesilkoy, F.; Arvelo, E.R.; Jahani, Y.; Liu, M.; Tittl, A.; Cevher, V.; Kivshar, Y.; Altug, H. Ultrasensitive hyperspectral imaging and biodetection enabled by dielectric metasurfaces. Nat. Photonics **2019**, 13, 390–396. [CrossRef]

103. Capocefalo, A.; Gentilini, S.; Barolo, L.; Baiocco, P.; Conti, C.; Ghofraniha, N. Biosensing with free space whispering gallery mode microlasers. Photonics Res. **2023**, 11, 732–741. [CrossRef]

104. Khmelevskaia, D.; Markina, D.I.; Fedorov, V.V.; Ermolaev, G.A.; Arsenin, A.V.; Volkov, V.S.; Goltaev, A.S.; Zadiranov, Y.M.; Tzibizov, I.A.; Pushkarev, A.P.; et al. Directly grown crystalline gallium phosphide on sapphire for nonlinear all-dielectric nanophotonics. Appl. Phys. Lett. **2021**, 118, 201101. [CrossRef]

105. Zhang, X.R.; Cui, T.J. Extensible on-chip mode manipulations based on metamaterials. Light Sci. Appl. **2022**, 11, 200. [CrossRef]

106. Salary, M.M.; Mosallaei, H. Tunable All-Dielectric Metasurfaces for Phase-Only Modulation of Transmitted Light Based on Quasi-bound States in the Continuum. ACS Photonics **2020**, 7, 1813–1829. [CrossRef]

107. Caldwell, J.D.; Lindsay, L.; Giannini, V.; Vurgaftman, I.; Reinecke, T.L.; Maier, S.A.; Glembocki, O.J. Low-loss, infrared and terahertz nanophotonics using surface phonon polaritons. Nanophotonics **2015**, 4, 44–68. [CrossRef]

108. Low, T.; Chaves, A.; Caldwell, J.D.; Kumar, A.; Fang, N.X.; Avouris, P.; Heinz, T.F.; Guinea, F.; Martin-Moreno, L.; Koppens, F. Polaritons in layered two-dimensional materials. Nat. Mater. **2017**, 16, 182–194. [CrossRef]

109. Dubrovkin, A.M.; Qiang, B.; Salim, T.; Nam, D.; Zheludev, N.I.; Wang, Q.J. Resonant nanostructures for highly confined and ultra-sensitive surface phonon-polaritons. Nat. Commun. **2020**, 11, 1863. [CrossRef]

110. Caldwell, J.D.; Glembocki, O.J.; Francescato, Y.; Sharac, N.; Giannini, V.; Bezares, F.J.; Long, J.P.; Owrutsky, J.C.; Vurgaftman, I.; Tischler, J.G.; et al. Low-loss, extreme subdiffraction photon confinement via silicon carbide localized surface phonon polariton resonators. Nano Lett. **2013**, 13, 3690–3697. [CrossRef]

111. Li, N.; Guo, X.; Yang, X.; Qi, R.; Qiao, T.; Li, Y.; Shi, R.; Li, Y.; Liu, K.; Xu, Z.; et al. Direct observation of highly confined phonon polaritons in suspended monolayer hexagonal boron nitride. Nat. Mater. **2021**, 20, 43–48. [CrossRef] [PubMed]

112. Hu, X.; Lo, T.W.; Mancini, A.; Gubbin, C.R.; Martini, F.; Zhang, J.; Gong, Z.M.; Politi, A.; De Liberato, S.; Zhang, X.F.; et al. Near-field nano-spectroscopy of strong mode coupling in phonon-polaritonic crystals. Appl. Phys. Rev. **2022**, 9, 021414. [CrossRef]

113. Yang, J.; Sun, Q.; Ueno, K.; Shi, X.; Oshikiri, T.; Misawa, H.; Gong, Q. Manipulation of the dephasing time by strong coupling between localized and propagating surface plasmon modes. Nat. Commun. **2018**, 9, 4858. [CrossRef] [PubMed]

114. Liu, K.; Huang, G.; Li, X.; Zhu, G.; Du, W.; Wang, T. Vibrational Strong Coupling between Surface Phonon Polaritons and Organic Molecules via Single Quartz Micropillars. Adv. Mater. **2022**, 34, e2109088. [CrossRef]

115. Yoo, D.; de León-Pérez, F.; Pelton, M.; Lee, I.-H.; Mohr, D.A.; Raschke, M.B.; Caldwell, J.D.; Martín-Moreno, L.; Oh, S.-H. Ultrastrong plasmon–phonon coupling via epsilon-near-zero nanocavities. Nat. Photonics **2020**, 15, 125–130. [CrossRef]

116. Amarie, S.; Keilmann, F. Broadband-infrared assessment of phonon resonance in scattering-type near-field microscopy. Phys. Rev. B **2011**, 83, 045404. [CrossRef]

117. Hasman, E.; Kleiner, V.; Dahan, N.; Gorodetski, Y.; Frischwasser, K.; Balin, I. Manipulation of Thermal Emission by Use of Micro and Nanoscale Structures. J. Heat Transf. **2012**, 134, 031023. [CrossRef]

118. Hillenbrand, R.; Taubner, T.; Keilmann, F. Phonon-enhanced light-matter interaction at the nanometre scale. Nature **2002**, 418, 159–162. [CrossRef]

119. Ma,W.; Hu, G.; Hu, D.; Chen, R.; Sun, T.; Zhang, X.; Dai, Q.; Zeng, Y.; Alu, A.; Qiu, C.W.; et al. Ghost hyperbolic surface polaritons in bulk anisotropic crystals. Nature **2021**, 596, 362–366. [CrossRef]

120. Oh, S.H.; Altug, H.; Jin, X.; Low, T.; Koester, S.J.; Ivanov, A.P.; Edel, J.B.; Avouris, P.; Strano, M.S. Nanophotonic biosensors harnessing van derWaals materials. Nat. Commun. **2021**, 12, 3824. [CrossRef]

121. Wang, Y.; Cui, Z.; Zhang, X.; Zhang, X.; Zhu, Y.; Chen, S.; Hu, H. Excitation of Surface Plasmon Resonance on Multiwalled Carbon Nanotube Metasurfaces for Pesticide Sensors. ACS Appl. Mater. Interfaces **2020**, 12, 52082–52088. [CrossRef] [PubMed]

122. Wang, R.Q.; Xu, W.D.; Chen, D.H.; Zhou, R.Y.; Wang, Q.; Gao, W.L.; Kono, J.; Xie, L.J.; Ying, Y.B. Ultrahigh-Sensitivity Molecular Sensing with Carbon Nanotube Terahertz Metamaterials. ACS Appl. Mater. Interfaces **2020**, 12, 40629–40634. [CrossRef]

123. Farmer, D.B.; Avouris, P.; Li, Y.; Heinz, T.F.; Han, S.-J. Ultrasensitive Plasmonic Detection of Molecules with Graphene. ACS Photonics **2016**, 3, 553–557. [CrossRef]

124. Boghossian, A.A.; Zhang, J.; Barone, P.W.; Reuel, N.F.; Kim, J.H.; Heller, D.A.; Ahn, J.H.; Hilmer, A.J.; Rwei, A.; Arkalgud, J.R.; et al.Near-infrared fluorescent sensors based on single-walled carbon nanotubes for life sciences applications. ChemSusChem **2011**, 4,

848–863. [CrossRef] [PubMed]

125. Zhang, J.; Landry, M.P.; Barone, P.W.; Kim, J.H.; Lin, S.; Ulissi, Z.W.; Lin, D.; Mu, B.; Boghossian, A.A.; Hilmer, A.J.; et al. Molecular recognition using corona phase complexes made of synthetic polymers adsorbed on carbon nanotubes. Nat. Nanotechnol. **2013**, 8,

959–968. [CrossRef]

126. Rodrigo, D.; Limaj, O.; Janner, D.; Etezadi, D.; Garcia de Abajo, F.J.; Pruneri, V.; Altug, H. Mid-infrared plasmonic biosensing with graphene. Science **2015**, 349, 165–168. [CrossRef]

127. Bareza, N.; Gopalan, K.K.; Alani, R.; Paulillo, B.; Pruneri, V. Mid-infrared Gas Sensing Using Graphene Plasmons Tuned by Reversible Chemical Doping. ACS Photonics **2020**, 7, 879–884. [CrossRef]

128. Hu, H.; Guo, X.D.; Hu, D.B.; Sun, Z.P.; Yang, X.X.; Dai, Q. Flexible and Electrically Tunable Plasmons in Graphene-Mica Heterostructures. Adv. Sci. **2018**, 5, 1800175. [CrossRef]

129. Hu, H.; Yang, X.; Zhai, F.; Hu, D.; Liu, R.; Liu, K.; Sun, Z.; Dai, Q. Far-field nanoscale infrared spectroscopy of vibrational fingerprints of molecules with graphene plasmons. Nat. Commun. **2016**, 7, 12334. [CrossRef]

130. Hu, H.; Yang, X.; Guo, X.; Khaliji, K.; Biswas, S.R.; Garcia de Abajo, F.J.; Low, T.; Sun, Z.; Dai, Q. Gas identification with graphene plasmons. Nat. Commun. **2019**, 10, 1131. [CrossRef]

131. Low, T.; Avouris, P. Graphene Plasmonics for Terahertz to Mid-Infrared Applications. ACS Nano **2014**, 8, 1086–1101. [CrossRef] [PubMed]

132. Rodrigo, D.; Tittl, A.; Limaj, O.; Abajo, F.J.G.; Pruneri, V.; Altug, H. Double-layer graphene for enhanced tunable infrared plasmonics. Light Sci. Appl. **2017**, 6, e16277. [CrossRef]

133. Jang, M.S.; Brar, V.W.; Sherrott, M.C.; Lopez, J.J.; Kim, L.; Kim, S.; Choi, M.; Atwater, midinfrared graphene Salisbury screen. Phys. Rev. B **2014**, 90, 165409. [CrossRef

134. Nong, J.; Tang, L.; Lan, G.; Luo, P.; Li, Z.; Huang, D.; Yi, J.; Shi, H.; Wei, W. Enhanced Graphene Plasmonic Mode Energy for Highly Sensitive Molecular Fingerprint Retrieval. Laser Photonics Rev. **2020**, 15, 2000300. [CrossRef]

135. Luxmoore, I.J.; Liu, P.Q.; Li, P.; Faist, J.; Nash, G.R. Graphene-Metamaterial Photodetectors for Integrated Infrared Sensing. ACS Photonics **2016**, 3, 936–941. [CrossRef]

136. Lee, I.H.; Yoo, D.; Avouris, P.; Low, T.; Oh, S.H. Graphene acoustic plasmon resonator for ultrasensitive infrared spectroscopy. Nat. Nanotechnol. **2019**, 14, 313–319. [CrossRef]

137. Guo, X.; Hu, H.; Liao, B.; Zhu, X.; Yang, X.; Dai, Q. Perfect-absorption graphene metamaterials for surface-enhanced molecular fingerprint spectroscopy. Nanotechnology **2018**, 29, 184004. [CrossRef]

138. Domino, K.L.; Khardikov, V.V.; Goryashko, V.; Nikitin, A.Y. Bonding and Antibonding Modes in Metal-Dielectric-Metal Plasmonic Antennas for Dual-Band Applications. Adv. Opt. Mater. **2020**, 8, 1900942. [CrossRef]

139. Ray, D.; Raziman, T.V.; Santschi, C.; Etezadi, D.; Altug, H.; Martin, O.J.F. Hybrid Metal-Dielectric Metasurfaces for Refractive Index Sensing. Nano Lett. **2020**, 20, 8752–8759. [CrossRef]

140. Huang, G.; Liu, K.; Shi, G.; Guo, Q.; Li, X.; Liu, Z.; Ma, W.; Wang, T. Elevating Surface-Enhanced Infrared Absorption with Quantum Mechanical Effects of Plasmonic Nanocavities. Nano Lett. **2022**, 22, 6083–6090. [CrossRef]

141. Pryce, I.M.; Kelaita, Y.A.; Aydin, K.; Atwater, H.A. Compliant Metamaterials for Resonantly Enhanced Infrared Absorption Spectroscopy and Refractive Index Sensing. ACS Nano **2011**, 5, 8167–8174. [CrossRef] [PubMed]

142. D'Andrea, C.; Bochterle, J.; Toma, A.; Huck, C.; Neubrech, F.; Messina, E.; Fazio, B.; Marago, O.M.; Di Fabrizio, E.; Lamy de La Chapelle, M.; et al. Optical nanoantennas for multiband surface-enhanced infrared and Raman spectroscopy. ACS Nano **2013**, 7,
3522–3531. [CrossRef] [PubMed]

143. Yoo, D.; Mohr, D.A.; Vidal-Codina, F.; John-Herpin, A.; Jo, M.; Kim, S.; Matson, J.; Caldwell, J.D.; Jeon, H.; Nguyen, N.-C.; et al. High-Contrast Infrared Absorption Spectroscopy via Mass-Produced Coaxial Zero-Mode Resonators with Sub-10 nm Gaps. Nano Lett. **2018**, 18, 1930–1936. [CrossRef] [PubMed]

144. Chen, X.; Ciraci, C.; Smith, D.R.; Oh, S.-H. Nanogap-Enhanced Infrared Spectroscopy with Template-Stripped Wafer-Scale Arrays of Buried Plasmonic Cavities. Nano Lett. **2015**, 15, 107–113. [CrossRef] [PubMed]

145. Dregely, D.; Neubrech, F.; Duan, H.; Vogelgesang, R.; Giessen, H. Vibrational near-field mapping of planar and buried threedimensional plasmonic nanostructures. Nat. Commun. **2013**, 4, 2237. [CrossRef]

146. Yoo, D.; Ngoc-Cuong, N.; Martin-Moreno, L.; Mohr, D.A.; Carretero-Palacios, S.; Shaver, J.; Peraire, J.; Ebbesen, T.W.; Oh, S.-H. High-Throughput Fabrication of Resonant Metamaterials with Ultrasmall Coaxial Apertures via Atomic Layer Lithography. Nano
Lett. **2016**, 16, 2040–2046. [CrossRef]

147. Yoo, D.; Vidal-Codina, F.; Ciraci, C.; Nguyen, N.C.; Smith, D.R.; Peraire, J.; Oh, S.H. Modeling and observation of mid-infrared nonlocality in effective epsilon-near-zero ultranarrow coaxial apertures. Nat. Commun. **2019**, 10, 4476. [CrossRef]

148. Oksenberg, E.; Shlesinger, I.; Tek, G.; Koenderink, A.F.; Garnett, E.C. Complementary Surface-Enhanced Raman Scattering (SERS) and IR Absorption Spectroscopy (SEIRAS) with Nanorods-on-a-Mirror. Adv. Funct. Mater. **2022**, 33, 2211154. [CrossRef]

149. Hu, X.; Xu, G.Q.;Wen, L.;Wang, H.C.; Zhao, Y.C.; Zhang, Y.X.; Cumming, D.R.S.; Chen, Q. Metamaterial absorber integrated microfluidic terahertz sensors. Laser Photonics Rev. **2016**, 10, 962–969. [CrossRef]

150. Le, T.H.H.; Tanaka, T. Plasmonics- Nanofluidics Hydrid Metamaterial: An Ultrasensitive Platform for Infrared Absorption Spectroscopy and Quantitative Measurement of Molecules. ACS Nano **2017**, 11, 9780–9788. [CrossRef]

151. Le, T.H.H.; Morita, A.; Mawatari, K.; Kitamori, T.; Tanaka, T. Metamaterials-Enhanced Infrared Spectroscopic Study of Nanoconfined Molecules by Plasmonics-Nanofluidics Hydrid Device. ACS Photonics **2018**, 5, 3179–3188. [CrossRef]

152. Miao, X.; Yan, L.; Wu, Y.; Liu, P.Q. High-sensitivity nanophotonic sensors with passive trapping of analyte molecules in hot spots.Light Sci. Appl. **2021**, 10, 5. [CrossRef] [PubMed]

153. Hasan, D.; Lee, C. Hybrid Metamaterial Absorber Platform for Sensing of CO2 Gas at Mid-IR. Adv. Sci. **2018**, 5, 1700581.[CrossRef] [PubMed]

154. Bareza, N., Jr.; Paulillo, B.; Slipchenko, T.M.; Autore, M.; Dolado, I.; Liu, S.; Edgar, J.H.; Vélez, S.; Martín-Moreno, L.;Hillenbrand, R.; et al. Phonon-Enhanced Mid-Infrared CO2 Gas Sensing Using Boron Nitride Nanoresonators. ACS Photonics
2022, 9, 34–42. [CrossRef]

155. Chong, X.Y.; Zhang, Y.J.; Li, E.W.; Kim, K.J.; Ohodnicki, P.R.; Chang, C.H.;Wang, A.X. Surface-Enhanced Infrared Absorption:Pushing the Frontier for On-Chip Gas Sensing. ACS Sens. **2018**, 3, 230–238. [CrossRef]

156. Zhou, H.; Hui, X.; Li, D.; Hu, D.; Chen, X.; He, X.; Gao, L.; Huang, H.; Lee, C.; Mu, X. Metal–Organic Framework-Surface-Enhanced Infrared Absorption Platform Enables Simultaneous On-Chip Sensing of Greenhouse Gases. Adv. Sci. **2020**, 7, 2001173. [CrossRef]

157. Zhou, H.; Ren, Z.; Xu, C.; Xu, L.; Lee, C. MOF/Polymer-Integrated Multi-Hotspot Mid-Infrared Nanoantennas for Sensitive Detection of CO(2) Gas. Nano-Micro Lett. **2022**, 14, 207. [CrossRef]

158. John-Herpin, A.; Tittl, A.; Altug, H. Quantifying the Limits of Detection of Surface-Enhanced Infrared Spectroscopy with Grating Order-Coupled Nanogap Antennas. ACS Photonics **2018**, 5, 4117–4124. [CrossRef]

159. Etezadi, D.; Warner, J.B.; Lashuel, H.A.; Altug, H. Real-Time In Situ Secondary Structure Analysis of Protein Monolayer with Mid-Infrared Plasmonic Nanoantennas. ACS Sens. **2018**, 3, 1109–1117. [CrossRef]

160. Han, J.H.; Lim, Y.C.; Kim, R.M.; Lv, J.; Cho, N.H.; Kim, H.; Namgung, S.D.; Im, S.W.; Nam, K.T. Neural-Network-Enabled Design of a Chiral Plasmonic Nanodimer for Target-Specific Chirality Sensing. ACS Nano **2023**, 17, 2306–2317. [CrossRef]

161. Ma, W.; Liu, Z.; Kudyshev, Z.A.; Boltasseva, A.; Cai, W.; Liu, Y. Deep learning for the design of photonic structures. Nat. Photonics **2020**, 15, 77–90. [CrossRef]

162. Kudyshev, Z.A.; Kildishev, A.V.; Shalaev, V.M.; Boltasseva, A. Machine-learning-assisted metasurface design for high-efficiency thermal emitter optimization. Appl. Phys. Rev. **2020**, 7, 021407. [CrossRef]

163. Malkiel, I.; Mrejen, M.; Nagler, A.; Arieli, U.;Wolf, L.; Suchowski, H. Plasmonic nanostructure design and characterization via Deep Learning. Light Sci. Appl. **2018**, 7, 60. [CrossRef] [PubMed]

164. Chen, M.K.; Liu, X.; Sun, Y.; Tsai, D.P. Artificial Intelligence in Meta-optics. Chem. Rev. **2022**, 122, 15356–15413. [CrossRef]

165. Zhou, H.; Xu, L.; Ren, Z.; Zhu, J.; Lee, C. Machine learning-augmented surface-enhanced spectroscopy toward next-generation molecular diagnostics. Nanoscale Adv. **2022**, 5, 538–570. [CrossRef]

166. Li, D.; Zhou, H.; Hui, X.; He, X.; Mu, X. Plasmonic Biosensor Augmented by a Genetic Algorithm for Ultra-Rapid, Label-Free, and Multi-Functional Detection of COVID-19. Anal. Chem. **2021**, 93, 9437–9444. [CrossRef]

167. Zhou, J.; Zhang, Z.; Dong, B.; Ren, Z.; Liu, W.; Lee, C. Midinfrared Spectroscopic Analysis of Aqueous Mixtures Using Artificial- Intelligence-Enhanced Metamaterial Waveguide Sensing Platform. ACS Nano **2023**, 17, 711–724. [CrossRef]

168. Hammiche, A.; Pollock, H.M.; Reading, M.; Claybourn, M.; Turner, P.H.; Jewkes, K. Photothermal FT-IR spectroscopy: A step towards FT-IR microscopy at a resolution better than the diffraction limit. Appl. Spectrosc. **1999**, 53, 810–815. [CrossRef]

169. Tanaka, T.; Yano, T.; Kato, R. Nanostructure-enhanced infrared spectroscopy. Nanophotonics **2022**, 11, 2541–2561. [CrossRef]

170. Anderson, M.S. Infrared spectroscopy with an atomic force microscope. Appl. Spectrosc. **2000**, 54, 349–352. [CrossRef]

171. Lu, F.; Jin, M.Z.; Belkin, M.A. Tip-enhanced infrared nanospectroscopy via molecular expansion force detection. Nat. Photonics **2014**, 8, 307–312. [CrossRef]

172. Xu, X.J.G.; Rang, M.; Craig, I.M.; Raschke, M.B. Pushing the Sample-Size Limit of Infrared Vibrational Nanospectroscopy: From Monolayer toward Single Molecule Sensitivity. J. Phys. Chem. Lett. **2012**, 3, 1836–1841. [CrossRef] [PubMed]

173. Almajhadi, M.A.; Uddin, S.M.A.;Wickramasinghe, H.K. Observation of nanoscale opto-mechanical molecular damping as the origin of spectroscopic contrast in photo induced force microscopy. Nat. Commun. **2020**, 11, 5691. [CrossRef] [PubMed]

174. Wei, J.; Li, Y.; Chang, Y.; Hasan, D.M.N.; Dong, B.; Ma, Y.; Qiu, C.W.; Lee, C. Ultrasensitive Transmissive Infrared Spectroscopy via Loss Engineering of Metallic Nanoantennas for Compact Devices. ACS Appl. Mater. Inter. **2019**, 11, 47270–47278. [CrossRef] [PubMed]

175. Pierce, J.R. Coupling of Modes of Propagation. J. Appl. Phys. **1954**, 25, 179–183. [CrossRef]

176. Miller, S.E. CoupledWave Theory and Waveguide Applications. Bell Syst. Tech. J. **1954**, 33, 661–719. [CrossRef]

177. Schelkunoff, S.A. Conversion of Maxwells Equations into Generalized Telegraphists Equations. Bell Syst. Tech. J. **1955**, 34, 995–1043. [CrossRef]

178. Haus, H.A. Waves and Fields in Optoelectronics; Prentice-Hall, Inc.: Upper Saddle River, NJ, USA, 1984.

179. Fan, S.; Suh, W.; Joannopoulos, J.D. Temporal coupled-mode theory for the Fano resonance in optical resonators. J. Opt. Soc. Am.A Opt. Image Sci. Vis. **2003**, 20, 569–572. [CrossRef]

180. Neuman, T.; Huck, C.; Vogt, J.; Neubrech, F.; Hillenbrand, R.; Aizpurua, J.; Pucci, A. Importance of Plasmonic Scattering for an Optimal Enhancement of Vibrational Absorption in SEIRA with Linear Metallic Antennas. J. Phys. Chem. C **2015**, 119, 26652–26662. [CrossRef]

181. Hwang, I.; Kim, M.; Yu, J.; Lee, J.; Choi, J.H.; Park, S.A.; Chang, W.S.; Lee, J.; Jung, J.Y. Ultrasensitive Molecule Detection Based on
Infrared Metamaterial Absorber with Vertical Nanogap. Small Methods **2021**, 5, e2100277. [CrossRef]

182. Zhou, H.; Li, D.; Ren, Z.; Mu, X.; Lee, C. Loss-induced phase transition in mid-infrared plasmonic metamaterials for ultrasensitive vibrational spectroscopy. InfoMat **2022**, 4, e12349. [CrossRef]

183. Aigner, A.; Tittl, A.; Wang, J.; Weber, T.; Kivshar, Y.; Maier, S.A.; Ren, H. Plasmonic bound states in the continuum to tailor light-matter coupling. Sci. Adv. **2022**, 8, eadd4816. [CrossRef] [PubMed]

184. Chen, X.; Wang, C.; Yao, Y.; Wang, C. Plasmonic Vertically Coupled Complementary Antennas for Dual-Mode Infrared Molecule Sensing. ACS Nano **2017**, 11, 8034–8046. [CrossRef]

185. Chang, Y.; Xu, S.; Dong, B.; Wei, J.; Le, X.; Ma, Y.; Zhou, G.; Lee, C. Development of triboelectric-enabled tunable Fabry-Pérot photonic-crystal-slab filter towards wearable mid-infrared computational spectrometer. Nano Energy **2021**, 89, 106446. [CrossRef]

186. Hasan, D.; Ho, C.P.; Lee, C. Realization of Fractal-Inspired Thermoresponsive Quasi-3D Plasmonic Metasurfaces with EOT-Like Transmission for Volumetric and Multispectral Detection in the Mid-IR Region. ACS Omega **2016**, 1, 818–831. [CrossRef] [PubMed]

187. Aouani, H.; Sipova, H.; Rahmani, M.; Navarro-Cia, M.; Hegnerova, K.; Homola, J.; Hong, M.; Maier, S.A. Ultrasensitive Broadband
Probing of Molecular Vibrational Modes with Multifrequency Optical Antennas. ACS Nano **2013**, 7, 669–675. [CrossRef]

188. Aslan, E.; Aslan, E.; Wang, R.; Hong, M.K.; Erramilli, S.; Turkmen, M.; Saracoglu, O.G.; Dal Negro, L. Multispectral Cesaro-Type Fractal Plasmonic Nanoantennas. ACS Photonics **2016**, 3, 2102–2111. [CrossRef]

189. Wu, C.; Khanikaev, A.B.; Adato, R.; Arju, N.; Yanik, A.A.; Altug, H.; Shvets, G. Fano-resonant asymmetric metamaterials for ultrasensitive spectroscopy and identification of molecular monolayers. Nat. Mater. **2012**, 11, 69–75. [CrossRef]

190. Rodrigo, D.; Tittl, A.; John-Herpin, A.; Limaj, O.; Altug, H. Self-Similar Multiresonant Nanoantenna Arrays for Sensing from Near- to Mid-Infrared. ACS Photonics **2018**, 5, 4903–4911. [CrossRef]

191. Gottheim, S.; Zhang, H.; Govorov, A.O.; Halas, N.J. Fractal Nanoparticle Plasmonics: The Cayley Tree. ACS Nano **2015**, 9, 3284–3292. [CrossRef]

192. Garoli, D.; Calandrini, E.; Bozzola, A.; Toma, A.; Cattarin, S.; Ortolani, M.; De Angelis, F. Fractal-Like Plasmonic Metamaterial with a Tailorable Plasma Frequency in the near-Infrared. ACS Photonics **2018**, 5, 3408–3414. [CrossRef]

193. Garoli, D.; Calandrini, E.; Bozzola, A.; Ortolani, M.; Cattarin, S.; Barison, S.; Toma, A.; De Angelis, F. Boosting infrared energy transfer in 3D nanoporous gold antennas. Nanoscale **2017**, 9, 915–922. [CrossRef]

194. Li, D.; Zhou, H.; Hui, X.; He, X.; Huang, H.; Zhang, J.;Mu, X.; Lee, C.; Yang, Y.Multifunctional Chemical Sensing Platform Based on Dual-Resonant Infrared Plasmonic Perfect Absorber for On-Chip Detection of Poly (ethyl cyanoacrylate). Adv. Sci. **2021**, 8, 2101879. [CrossRef] [PubMed]

195. Yang, J.; Hu, X.; Li, X.; Liu, Z.; Liang, Z.; Jiang, X.; Zi, J. Broadband absorption enhancement in anisotropic metamaterials by mirror reflections. Phys. Rev. B **2009**, 80, 125103. [CrossRef]

196. Cui, Y.; Fung, K.H.; Xu, J.; Ma, H.; Jin, Y.; He, S.; Fang, N.X. Ultrabroadband light absorption by a sawtooth anisotropic metamaterial slab. Nano Lett. **2012**, 12, 1443–1447. [CrossRef] [PubMed]

197. Hegde, R.S. Deep learning: A new tool for photonic nanostructure design. Nanoscale Adv. **2020**, 2, 1007–1023. [CrossRef]

198. Jiang, Z.H.; Yun, S.; Toor, F.;Werner, D.H.; Mayer, T.S. Conformal Dual-Band Near-Perfectly Absorbing Mid-Infrared Metamaterial Coating. ACS Nano **2011**, 5, 4641–4647. [CrossRef]

199. Bossard, J.A.; Lin, L.; Yun, S.; Liu, L.;Werner, D.H.; Mayer, T.S. Near-Ideal Optical Metamaterial Absorbers with Super-Octave Bandwidth. ACS Nano **2014**, 8, 1517–1524. [CrossRef]

200. Yeung, C.; Tsai, J.-M.; King, B.; Pham, B.; Ho, D.; Liang, J.; Knight, M.W.; Raman, A.P. Multiplexed supercell metasurface design and optimization with tandem residual networks. Nanophotonics **2021**, 10, 1133–1143. [CrossRef]

201. Maniyara, R.A.; Rodrigo, D.; Yu, R.; Canet-Ferrer, J.; Ghosh, D.S.; Yongsunthon, R.; Baker, D.E.; Rezikyan, A.; García de Abajo, F.J.; Pruneri, V. Tunable plasmons in ultrathin metal films. Nat. Photonics **2019**, 13, 328–333. [CrossRef]

202. Wu, C.; Guo, X.; Duan, Y.; Lyu, W.; Hu, H.; Hu, D.; Chen, K.; Sun, Z.; Gao, T.; Yang, X.; et al. Ultrasensitive Mid-Infrared Biosensing in Aqueous Solutions with Graphene Plasmons. Adv. Mater. **2022**, 34, e2110525. [CrossRef]

203. Karst, J.; Floess, M.; Ubl, M.; Dingler, C.; Malacrida, C.; Steinle, T.; Ludwigs, S.; Hentschel, M.; Giessen, H. Electrically switchable metallic polymer nanoantennas. Science **2021**, 374, 612–616. [CrossRef] [PubMed]

204. Chen, R.T.; Nguyen, H.; Wu, M.C. A low voltage micromachined optical switch by stress-induced bending. In Proceedings of the Technical Digest. IEEE International MEMS 99 Conference. Twelfth IEEE International Conference on Micro Electro Mechanical Systems (Cat. No.99CH36291), Orlando, FL, USA, 21–21 January 1999; pp. 424–428. [CrossRef]

205. Lee, C. Monolithic-integrated 8CH MEMS variable optical attenuators. Sens. Actuators A Phys. **2005**, 123–124, 596–601. [CrossRef]

206. Lu, C. Foundation of MEMS; Pearson: London, UK, 2012; Volume 66, pp. 37–39.

207. Ren, Z.; Chang, Y.; Ma, Y.; Shih, K.; Dong, B.; Lee, C. Leveraging of MEMS Technologies for Optical Metamaterials Applications. Adv. Opt. Mater. **2020**, 8, 1900653. [CrossRef]

208. Xu, J.; Du, Y.; Tian, Y.;Wang, C. Progress in wafer bonding technology towards MEMS, high-power electronics, optoelectronics, and optofluidics. Int. J. Optomechatron. **2020**, 14, 94–118. [CrossRef]

209. Pitchappa, P.; Kumar, A.; Singh, R.; Lee, C.; Wang, N. Terahertz MEMS metadevices. J. Micromech. Microeng. **2021**, 31, 113001. [CrossRef]

210. Zhou, G.; Lim, Z.H.; Qi, Y.; Chau, F.S.; Zhou, G. MEMS gratings and their applications. Int. J. Optomechatron. **2021**, 15, 61–86. [CrossRef]

211. Le, X.; Shi, Q.; Vachon, P.; Ng, E.J.; Lee, C. Piezoelectric MEMS—Evolution from sensing technology to diversified applications in the 5G/Internet of Things (IoT) era. J. Micromech. Microeng. **2022**, 32, 014005. [CrossRef]

212. Liu, X.; Qiao, Q.; Dong, B.; Liu, W.; Xu, C.; Xu, S.; Zhou, G. MEMS enabled suspended silicon waveguide platform for long-wave infrared modulation applications. Int. J. Optomechatron. **2022**, 16, 42–57. [CrossRef]

213. Xu, C.; Ren, Z.;Wei, J.; Lee, C. Reconfigurable terahertz metamaterials: From fundamental principles to advanced 6G applications. iScience **2022**, 25, 103799. [CrossRef]

214. Wang, D.;Watkins, C.; Xie, H. MEMS Mirrors for LiDAR: A review. Micromachines **2020**, 11, 456. [CrossRef]

215. Qian, Z.; Kang, S.; Rajaram, V.; Cassella, C.; McGruer, N.E.; Rinaldi, M. Zero-power infrared digitizers based on plasmonically enhanced micromechanical photoswitches. Nat. Nanotechnol. **2017**, 12, 969–973. [CrossRef]

216. Zhou, G.; Lee, C. Optical MEMS, Nanophotonics, and Their Applications; CRC Press: Boca Raton, FL, USA, 2017; pp. 1–432.

217. Xu, R.; Lin, Y.-S. Flexible and Controllable Metadevice Using Self-Assembly MEMS Actuator. Nano Lett. **2021**, 21, 3205–3210. [CrossRef]

218. Xu, R.; Xu, X.; Yang, B.-R.; Gui, X.; Qin, Z.; Lin, Y.-S. Actively logical modulation of MEMS-based terahertz metamaterial. Photonics Res. **2021**, 9, 1409. [CrossRef]

219. Pitchappa, P.; Ho, C.P.; Dhakar, L.; Qian, Y.; Singh, N.; Lee, C. Periodic Array of Subwavelength MEMS Cantilevers for Dynamic Manipulation of Terahertz Waves. J. Microelectromech. Syst. **2015**, 24, 525–527. [CrossRef]

220. Pitchappa, P.; Manjappa, M.; Ho, C.P.; Singh, R.; Singh, N.; Lee, C. Active Control of Electromagnetically Induced Transparency Analog in Terahertz MEMS Metamaterial. Adv. Opt. Mater. **2016**, 4, 541–547. [CrossRef]

221. Cong, L.; Pitchappa, P.; Wu, Y.; Ke, L.; Lee, C.; Singh, N.; Yang, H.; Singh, R. Active Multifunctional Microelectromechanical SystemMetadevices: Applications in Polarization Control,Wavefront Deflection, and Holograms. Adv. Opt. Mater. **2017**, 5, 1600716. [CrossRef]

222. Pitchappa, P.; Ho, C.P.; Cong, L.; Singh, R.; Singh, N.; Lee, C. Reconfigurable Digital Metamaterial for Dynamic Switching of Terahertz Anisotropy. Adv. Opt. Mater. **2016**, 4, 391–398. [CrossRef]

223. Pitchappa, P.; Manjappa, M.; Ho, C.P.; Qian, Y.; Singh, R.; Singh, N.; Lee, C. Active control of near-field coupling in conductively coupled microelectromechanical system metamaterial devices. Appl. Phys. Lett. **2016**, 108, 111102. [CrossRef]

224. Shih, K.; Pitchappa, P.; Manjappa, M.; Ho, C.P.; Singh, R.; Yang, B.; Singh, N.; Lee, C. Active MEMS metamaterials for THz bandwidth control. Appl. Phys. Lett. **2017**, 110, 161108. [CrossRef]

225. Manjappa, M.; Pitchappa, P.;Wang, N.; Lee, C.; Singh, R. Active Control of Resonant Cloaking in a Terahertz MEMS Metamaterial. Adv. Opt. Mater. **2018**, 6, 1800141. [CrossRef]

226. Cong, L.; Pitchappa, P.; Lee, C.; Singh, R. Active Phase Transition via Loss Engineering in a Terahertz MEMS Metamaterial. Adv. Mater. **2017**, 29, 1700733. [CrossRef] [PubMed]

227. Manjappa, M.; Pitchappa, P.; Singh, N.;Wang, N.; Zheludev, N.I.; Lee, C.; Singh, R. Reconfigurable MEMS Fano metasurfaces with multiple-input–output states for logic operations at terahertz frequencies. Nat. Commun. **2018**, 9, 4056. [CrossRef] [PubMed]

228. Pitchappa, P.; Manjappa, M.; Krishnamoorthy, H.N.S.; Chang, Y.; Lee, C.; Singh, R. Bidirectional reconfiguration and thermal tuning of microcantilever metamaterial device operating from 77 K to 400 K. Appl. Phys. Lett. **2017**, 111, 261101. [CrossRef]

229. Cong, L.; Singh, R. Spatiotemporal Dielectric Metasurfaces for Unidirectional Propagation and Reconfigurable Steering of Terahertz Beams. Adv. Mater. **2020**, 32, 2001418. [CrossRef]

230. Cong, L.; Srivastava, Y.K.; Zhang, H.; Zhang, X.; Han, J.; Singh, R. All-optical active THz metasurfaces for ultrafast polarization switching and dynamic beam splitting. Light Sci. Appl. **2018**, 7, 28. [CrossRef]

231. Tan, T.C.; Srivastava, Y.K.; Ako, R.T.; Wang, W.; Bhaskaran, M.; Sriram, S.; Al-Naib, I.; Plum, E.; Singh, R. Active Control of Nanodielectric-Induced THz Quasi-BIC in Flexible Metasurfaces: A Platform for Modulation and Sensing. Adv. Mater. **2021**, 33, 2100836. [CrossRef]

232. Agarwal, P.; Medwal, R.; Kumar, A.; Asada, H.; Fukuma, Y.; Rawat, R.S.; Battiato, M.; Singh, R. Ultrafast Photo-Thermal Switching of Terahertz Spin Currents. Adv. Funct. Mater. **2021**, 31, 2010453. [CrossRef]

233. Pitchappa, P.; Kumar, A.; Prakash, S.; Jani, H.; Venkatesan, T.; Singh, R. Chalcogenide Phase Change Material for Active Terahertz Photonics. Adv. Mater. **2019**, 31, 1808157. [CrossRef]

234. Pitchappa, P.; Kumar, A.; Liang, H.; Prakash, S.; Wang, N.; Bettiol, A.A.; Venkatesan, T.; Lee, C.; Singh, R. Frequency-Agile Temporal Terahertz Metamaterials. Adv. Opt. Mater. **2020**, 8, 2000101. [CrossRef]

235. Cong, L.; Pitchappa, P.; Wang, N.; Singh, R. Electrically Programmable Terahertz Diatomic Metamolecules for Chiral Optical Control. Research **2019**, 2019, 7084251. [CrossRef] [PubMed]

236. Chen, S.; Liu, Z.; Du, H.; Tang, C.; Ji, C.Y.; Quan, B.; Pan, R.; Yang, L.; Li, X.; Gu, C.; et al. Electromechanically reconfigurable optical nano-kirigami. Nat. Commun. **2021**, 12, 1299. [CrossRef] [PubMed]

237. Kuball, H.-G. Circular Dichroism and Linear Dichroism. Z. Phys. Chem. **1999**, 212, 118–119. [CrossRef]

238. Govorov, A.O.; Fan, Z.; Hernandez, P.; Slocik, J.M.; Naik, R.R. Theory of Circular Dichroism of Nanomaterials Comprising Chiral Molecules and Nanocrystals: Plasmon Enhancement, Dipole Interactions, and Dielectric Effects. Nano Lett. **2010**, 10, 1374–1382. [CrossRef] [PubMed]

239. Liu, Z.; Du, H.; Li, J.; Lu, L.; Li, Z.-Y.; Fang, N.X. Nano-kirigami with giant optical chirality. Sci. Adv. **2018**, 4, eaat4436. [CrossRef] [PubMed]

240. Kwon, H.; Faraon, A. NEMS-Tunable Dielectric Chiral Metasurfaces. ACS Photonics **2021**, 8, 2980–2986. [CrossRef]

241. Kwon, H.; Zheng, T.; Faraon, A. Nano-electromechanical Tuning of Dual-Mode Resonant Dielectric Metasurfaces for Dynamic Amplitude and Phase Modulation. Nano Lett. **2021**, 21, 2817–2823. [CrossRef]

242. Yang, X.; Zhao, X.; Yang, K.; Liu, Y.; Liu, Y.; Fu, W.; Luo, Y. Biomedical Applications of Terahertz Spectroscopy and Imaging. Trends Biotechnol. **2016**, 34, 810–824. [CrossRef]

243. Zhu, Y.; Li, Z.; Hao, Z.; DiMarco, C.; Maturavongsadit, P.; Hao, Y.; Lu, M.; Stein, A.; Wang, Q.; Hone, J.; et al. Optical conductivity-based ultrasensitive mid-infrared biosensing on a hybrid metasurface. Light Sci. Appl. **2018**, 7, 67. [CrossRef]

244. Kühner, L.; Semenyshyn, R.; Hentschel, M.; Neubrech, F.; Tarín, C.; Giessen, H. Vibrational Sensing Using Infrared Nanoantennas: Toward the Noninvasive Quantitation of Physiological Levels of Glucose and Fructose. ACS Sens. **2019**, 4, 1973–1979. [CrossRef]

245. Byler, D.M.; Susi, H. Examination of the secondary structure of proteins by deconvolved FTIR spectra. Biopolymers **1986**, 25, 469–487. [CrossRef] [PubMed]

246. Soto, C.; Pritzkow, S. Protein misfolding, aggregation, and conformational strains in neurodegenerative diseases. Nat. Neurosci. **2018**, 21, 1332–1340. [CrossRef] [PubMed]

247. Aslam, N.; Pfender, M.; Neumann, P.; Reuter, R.; Zappe, A.; Fávaro de Oliveira, F.; Denisenko, A.; Sumiya, H.; Onoda, S.; Isoya, J.; et al. Nanoscale nuclear magnetic resonance with chemical resolution. Science **2017**, 357, 67–71. [CrossRef]

248. Amenabar, I.; Poly, S.; Nuansing, W.; Hubrich, E.H.; Govyadinov, A.A.; Huth, F.; Krutokhvostov, R.; Zhang, L.; Knez, M.; Heberle, J.; et al. Structural analysis and mapping of individual protein complexes by infrared nanospectroscopy. Nat. Commun. **2013**, 4, 2890. [CrossRef] [PubMed]

249. Boutet, S.; Lomb, L.; Williams, G.J.; Barends, T.R.M.; Aquila, A.; Doak, R.B.; Weierstall, U.; DePonte, D.P.; Steinbrener, J.; Shoeman, R.L.; et al. High-resolution protein structure determination by serial femtosecond crystallography. Science **2012**, 337, 362–364. [CrossRef]

250. Semenyshyn, R.; Hentschel, M.; Stanglmair, C.; Teutsch, T.; Tarin, C.; Pacholski, C.; Giessen, H.; Neubrech, F. In Vitro Monitoring Conformational Changes of Polypeptide Monolayers Using Infrared Plasmonic Nanoantennas. Nano Lett. **2019**, 19, 1–7. [CrossRef]

251. Hinkov, B.; Pilat, F.; Lux, L.; Souza, P.L.; David, M.; Schwaighofer, A.; Ristani´c, D.; Schwarz, B.; Detz, H.; Andrews, A.M.; et al. A mid-infrared lab-on-a-chip for dynamic reaction monitoring. Nat. Commun. **2022**, 13, 4753. [CrossRef]

252. Hendry, E.; Carpy, T.; Johnston, J.; Popland, M.; Mikhaylovskiy, R.V.; Lapthorn, A.J.; Kelly, S.M.; Barron, L.D.; Gadegaard, N.; Kadodwala, M. Ultrasensitive detection and characterization of biomolecules using superchiral fields. Nat. Nanotechnol. **2010**, 5, 783–787. [CrossRef]

253. Probst, P.T.; Mayer, M.; Gupta, V.; Steiner, A.M.; Zhou, Z.; Auernhammer, G.K.; König, T.A.F.; Fery, A. Mechano-tunable chiral metasurfaces via colloidal assembly. Nat. Mater. **2021**, 20, 1024–1028. [CrossRef]

254. Cunningham, B.T.; Zhang, M.; Zhuo, Y.; Kwon, L.; Race, C. Recent Advances in Biosensing with Photonic Crystal Surfaces: A Review. IEEE Sens. J. **2016**, 16, 3349–3366. [CrossRef]

255. Domenici, F.; Capocefalo, A.; Brasili, F.; Bedini, A.; Giliberti, C.; Palomba, R.; Silvestri, I.; Scarpa, S.;Morrone, S.; Paradossi, G.; et al. Ultrasound delivery of Surface Enhanced InfraRed Absorption active gold-nanoprobes into fibroblast cells: A biological study via Synchrotron-based InfraRed microanalysis at single cell level. Sci. Rep. **2019**, 9, 11845. [CrossRef] [PubMed]

256. Capocefalo, A.; Mammucari, D.; Brasili, F.; Fasolato, C.; Bordi, F.; Postorino, P.; Domenici, F. Exploring the Potentiality of a SERS-Active pH Nano-Biosensor. Front. Chem. **2019**, 7, 413. [CrossRef] [PubMed]

257. Fasolato, C.; Giantulli, S.; Capocefalo, A.; Toumia, Y.; Notariello, D.; Mazzarda, F.; Silvestri, I.; Postorino, P.; Domenici, F. Antifolate SERS-active nanovectors: Quantitative drug nanostructuring and selective cell targeting for effective theranostics. Nanoscale **2019**, 11, 15224–15233. [CrossRef]

258. Zhou, R.; Wang, C.; Huang, Y.; Huang, K.; Wang, Y.; Xu, W.; Xie, L.; Ying, Y. Label-free terahertz microfluidic biosensor for sensitive DNA detection using graphene-metasurface hybrid structures. Biosens. Bioelectron. **2021**, 188, 113336. [CrossRef]

259. Bai, Z.; Liu, Y.; Kong, R.; Nie, T.; Sun, Y.; Li, H.; Sun, T.; Pandey, C.;Wang, Y.; Zhang, H.; et al. Near-field Terahertz Sensing of Hela cells and Pseudomonas Based on Monolithic Integrated Metamaterials with Spintronic Terahertz Emitter. ACS Appl. Mater. Interfaces **2020**, 12, 35895–35902. [CrossRef]

260. Ahmadivand, A.; Gerislioglu, B.; Ramezani, Z.; Kaushik, A.; Manickam, P.; Ghoreishi, S.A. Functionalized terahertz plasmonic metasensors: Femtomolar-level detection of SARS-CoV-2 spike proteins. Biosens. Bioelectron. **2021**, 177, 112971. [CrossRef] [PubMed]

261. Tenggara, A.P.; Park, S.J.; Yudistira, H.T.; Ahn, Y.H.; Byun, D. Fabrication of terahertz metamaterials using electrohydrodynamic jet printing for sensitive detection of yeast. J. Micromech. Microeng. **2017**, 27, 035009. [CrossRef]

262. Shih, K.; Pitchappa, P.; Jin, L.; Chen, C.-H.; Singh, R.; Lee, C. Nanofluidic terahertz metasensor for sensing in aqueous environment. Appl. Phys. Lett. **2018**, 113, 071105. [CrossRef]

263. Shih, K.; Pitchappa, P.; Manjappa, M.; Ho, C.P.; Singh, R.; Lee, C. Microfluidic metamaterial sensor: Selective trapping and remote sensing of microparticles. J. Appl. Phys. **2017**, 121, 023102. [CrossRef]

264. Park, H.-R.; Ahn, K.J.; Han, S.; Bahk, Y.-M.; Park, N.; Kim, D.-S. Colossal Absorption of Molecules Inside Single Terahertz Nanoantennas. Nano Lett. **2013**, 13, 1782–1786. [CrossRef]

265. Fanget, S.; Hentz, S.; Puget, P.; Arcamone, J.; Matheron, M.; Colinet, E.; Andreucci, P.; Duraffourg, L.; Myers, E.; Roukes, M.L. Gas sensors based on gravimetric detection—A review. Sens. Actuators B Chem. **2011**, 160, 804–821. [CrossRef]

266. Gutmacher, D.; Hoefer, U.; Wöllenstein, J. Gas sensor technologies for fire detection. Sens. Actuators B Chem. **2012**, 175, 40–45. [CrossRef]

267. Liu, W.; Ma, Y.; Liu, X.; Zhou, J.; Xu, C.; Dong, B.; Lee, C. Larger-Than-Unity External Optical Field Confinement Enabled by Metamaterial-Assisted Comb Waveguide for Ultrasensitive Long-Wave Infrared Gas Spectroscopy. Nano Lett. **2022**, 22, 6112–6120.
[CrossRef]

268. Liu, W.; Ma, Y.; Chang, Y.; Dong, B.; Wei, J.; Ren, Z.; Lee, C. Suspended silicon waveguide platform with subwavelength grating metamaterial cladding for long-wave infrared sensing applications. Nanophotonics **2021**, 10, 1861–1870. [CrossRef]

269. Davies, S.J.; Španˇel, P.; Smith, D. Breath analysis of ammonia, volatile organic compounds and deuterated water vapor in chronic kidney disease and during dialysis. Bioanalysis **2014**, 6, 843–857. [CrossRef]

270. Huber, M.; Kepesidis, K.V.; Voronina, L.; Boži´c, M.; Trubetskov, M.; Harbeck, N.; Krausz, F.; Žigman, M. Stability of person-specific blood-based infrared molecular fingerprints opens up prospects for health monitoring. Nat. Commun. **2021**, 12, 1511. [CrossRef]

271. Arasaradnam, R.P.; Covington, J.A.; Harmston, C.; Nwokolo, C.U. Review article: Next generation diagnostic modalities in gastroenterology-gas phase volatile compound biomarker detection. Aliment. Pharmacol. Ther. **2014**, 39, 780–789. [CrossRef]

272. Chang, Y.C.; Wagli, P.; Paeder, V.; Homsy, A.; Hvozdara, L.; van der Wal, P.; Di Francesco, J.; de Rooij, N.F.; Peter Herzig, H.Cocaine detection by a mid-infrared waveguide integrated with a microfluidic chip. Lab Chip **2012**, 12, 3020–3023. [CrossRef]

273. Lim, Z.H.; Qi, Y.; Zhou, G.; Senthil Kumar, A.; Lee, C.; Zhou, G. Cascaded, self-calibrated, single-pixel mid-infrared Hadamard transform spectrometer. Opt. Express **2021**, 29, 34600–34615. [CrossRef]

274. Sabry, Y.M.; Khalil, D.; Bourouina, T. Monolithic silicon-micromachined free-space optical interferometers onchip. Laser Photonics Rev. **2015**, 9, 1–24. [CrossRef]

275. Tang, Y.; Cohen, A.E. Optical Chirality and Its Interaction with Matter. Phys. Rev. Lett. **2010**, 104, 163901. [CrossRef]

276. Naaman, R.; Paltiel, Y.;Waldeck, D.H. Chiral molecules and the electron spin. Nat. Rev. Chem. **2019**, 3, 250–260. [CrossRef]

277. Ariëns, E.J. Stereochemistry, a basis for sophisticated nonsense in pharmacokinetics and clinical pharmacology. Eur. J. Clin.
Pharmacol. **1984**, 26, 663–668. [CrossRef]

278. Nickerson, B.; Salisbury, J.J.; Harwood, J.W. Enantioselective analysis for L-pidolic acid in ertugliflozin drug substance and drug product by chiral gas chromatography with derivatization. J. Pharm. Biomed. Anal. **2018**, 159, 212–216. [CrossRef] [PubMed]

279. Zhang, L.; Wan, S.; Jiang, Y.; Wang, Y.; Fu, T.; Liu, Q.; Cao, Z.; Qiu, L.; Tan, W. Molecular Elucidation of Disease Biomarkers at the Interface of Chemistry and Biology. J. Am. Chem. Soc. **2017**, 139, 2532–2540. [CrossRef] [PubMed]

280. Tang, Y.; Cohen, A.E. Enhanced Enantioselectivity in Excitation of Chiral Molecules by Superchiral Light. Science **2011**, 332, 333–336. [CrossRef]

281. Chen, Y.; Deng, H.; Sha, X.; Chen, W.;Wang, R.; Chen, Y.H.;Wu, D.; Chu, J.; Kivshar, Y.S.; Xiao, S.; et al. Observation of intrinsic chiral bound states in the continuum. Nature **2023**, 613, 474–478. [CrossRef]

282. Vázquez-Guardado, A.; Chanda, D. Superchiral Light Generation on Degenerate Achiral Surfaces. Phys. Rev. Lett. **2018**, 120, 137601. [CrossRef]

283. Zhao, Y.; Askarpour, A.N.; Sun, L.; Shi, J.; Li, X.; Alù, A. Chirality detection of enantiomers using twisted optical metamaterials. Nat. Commun. **2017**, 8, 14180. [CrossRef]

284. Cen, M.; Wang, J.; Liu, J.; He, H.; Li, K.; Cai, W.; Cao, T.; Liu, Y.J. Ultrathin Suspended Chiral Metasurfaces for Enantiodiscrimination. Adv. Mater. **2022**, 34, e2203956. [CrossRef]

285. Han, Z.; Wang, F.; Sun, J.; Wang, X.; Tang, Z. Recent Advances in Ultrathin Chiral Metasurfaces by Twisted Stacking. Adv. Mater. **2023**, 35, e2206141. [CrossRef] [PubMed]

286. Kakkar, T.; Keijzer, C.; Rodier, M.; Bukharova, T.; Taliansky, M.; Love, A.J.; Milner, J.J.; Karimullah, A.S.; Barron, L.D.; Gadegaard, N.; et al. Superchiral near fields detect virus structure. Light Sci. Appl. **2020**, 9, 195. [CrossRef] [PubMed]

287. Baumruk, V.; Keiderling, T.A. Vibrational circular dichroism of proteins in water solution. J. Am. Chem. Soc. **1993**, 115, 6939–6942. [CrossRef]

288. Iida, T.; Ishikawa, A.; Tanaka, T.; Muranaka, A.; Uchiyama, M.; Hayashi, Y.; Tsuruta, K. Super-chiral vibrational spectroscopy with metasurfaces for high-sensitive identification of alanine enantiomers. Appl. Phys. Lett. **2020**, 117, 101103. [CrossRef]

289. Knipper, R.; Kopecký, V.; Huebner, U.; Popp, J.; Mayerhöfer, T.G. Slit-Enhanced Chiral- and Broadband Infrared Ultra-Sensing. ACS Photonics **2018**, 5, 3238–3245. [CrossRef]

290. Shanmugam, G.; Polavarapu, P.L. Vibrational circular dichroism spectra of protein films: Thermal denaturation of bovine serum albumin. Biophys. Chem. **2004**, 111, 73–77. [CrossRef]

291. Hassan, D.S.; Wolf, C. Optical deciphering of multinary chiral compound mixtures through organic reaction based chemometric chirality sensing. Nat. Commun. **2021**, 12, 6451. [CrossRef]

292. Xu, C.; Ren, Z.; Zhou, H.; Zhou, J.; Ho, C.P.; Wang, N.; Lee, C. Expanding chiral metamaterials for retrieving fingerprints via vibrational circular dichroism. Light Sci. Appl. **2023**, 12, 154. [CrossRef]

293. Xiao, T.-H.; Cheng, Z.; Luo, Z.; Isozaki, A.; Hiramatsu, K.; Itoh, T.; Nomura, M.; Iwamoto, S.; Goda, K. All-dielectric chiral-fieldenhanced Raman optical activity. Nat. Commun. **2021**, 12, 3062. [CrossRef]

294. Krupová, M.; Kessler, J.; Bouˇr, P. Recent Trends in Chiroptical Spectroscopy: Theory and Applications of Vibrational Circular Dichroism and Raman Optical Activity. ChemPlusChem **2020**, 85, 561–575. [CrossRef]

295. Zhang, W.; Ai, B.; Gu, P.; Guan, Y.; Wang, Z.; Xiao, Z.; Zhang, G. Plasmonic Chiral Metamaterials with Sub-10 nm Nanogaps. ACS Nano **2021**, 15, 17657–17667. [CrossRef] [PubMed]

296. Choi,W.J.; Yano, K.; Cha, M.; Colombari, F.M.; Kim, J.-Y.; Wang, Y.; Lee, S.H.; Sun, K.; Kruger, J.M.; de Moura, A.F.; et al. Chiral phonons in microcrystals and nanofibrils of biomolecules. Nat. Photonics **2022**, 16, 366–373. [CrossRef]

297. Choi, W.J.; Lee, S.H.; Park, B.C.; Kotov, N.A. Terahertz Circular Dichroism Spectroscopy of Molecular Assemblies and Nanostructures. J. Am. Chem. Soc. **2022**, 144, 22789–22804. [CrossRef] [PubMed]

298. Choi,W.J.; Cheng, G.; Huang, Z.; Zhang, S.; Norris, T.B.; Kotov, N.A. Terahertz circular dichroism spectroscopy of biomaterials enabled by kirigami polarization modulators. Nat. Mater. **2019**, 18, 820–826. [CrossRef]

299. McDonnell, C.; Deng, J.; Sideris, S.; Ellenbogen, T.; Li, G. Functional THz emitters based on Pancharatnam-Berry phase nonlinear metasurfaces. Nat. Commun. **2021**, 12, 30. [CrossRef]

300. Zhang, M.; Hao, D.; Wang, S.; Li, R.; Wang, S.; Ma, Y.; Moro, R.; Ma, L. Chiral biosensing using terahertz twisted chiral metamaterial. Opt. Express **2022**, 30, 14651–14660. [CrossRef] [PubMed]

301. Dong, B.; Zhang, Z.; Shi, Q.; Wei, J.; Ma, Y.; Xiao, Z.; Lee, C. Biometrics-protected optical communication enabled by deep learning–enhanced triboelectric/photonic synergistic interface. Sci. Adv. **2022**, 8, eabl9874. [CrossRef]

302. Huang, L.; Dong, B.; Yu, Z.G.; Zhou, J.; Ma, Y.; Zhang, Y.-W.; Lee, C.; Ang, K.-W. Mid-infrared modulators integrating silicon and black phosphorus photonics. Mater. Today Adv. **2021**, 12, 100170. [CrossRef]

303. Liu, X.; Liu, W.; Ren, Z.; Ma, Y.; Dong, B.; Zhou, G.; Lee, C. Progress of optomechanical micro/nano sensors: A review. Int. J. Optomechatronics **2021**, 15, 120–159. [CrossRef]

304. Ma, Y.; Dong, B.; Lee, C. Progress of infrared guided-wave nanophotonic sensors and devices. Nano Converg. **2020**, 7, 12. [CrossRef]

305. Zhu, J.; Sun, Z.; Xu, J.;Walczak, R.D.; Dziuban, J.A.; Lee, C. Volatile organic compounds sensing based on Bennet doubler-inspired triboelectric nanogenerator and machine learning-assisted ion mobility analysis. Sci. Bull. **2021**, 66, 1176–1185. [CrossRef]
[PubMed]

306. Chang, Y.; Wei, J.; Lee, C. Metamaterials–from fundamentals and MEMS tuning mechanisms to applications. Nanophotonics **2020**, 9, 3049–3070. [CrossRef]

307. Jahani, Y.; Arvelo, E.R.; Yesilkoy, F.; Koshelev, K.; Cianciaruso, C.; De Palma, M.; Kivshar, Y.; Altug, H. Imaging-based spectrometerless optofluidic biosensors based on dielectric metasurfaces for detecting extracellular vesicles. Nat. Commun. **2021**, 12, 3246.
[CrossRef]

308. Wei, J.; Li, Y.; Wang, L.; Liao, W.; Dong, B.; Xu, C.; Zhu, C.; Ang, K.W.; Qiu, C.W.; Lee, C. Zero-bias mid-infrared graphene photodetectors with bulk photoresponse and calibration-free polarization detection. Nat. Commun. **2020**, 11, 6404. [CrossRef]
[PubMed]

309. Wei, J.; Xu, C.; Dong, B.; Qiu, C.-W.; Lee, C. Mid-infrared semimetal polarization detectors with configurable polarity transition. Nat. Photonics **2021**, 15, 614–621. [CrossRef]

310. Wei, J.; Chen, Y.; Li, Y.; Li, W.; Xie, J.; Lee, C.; Novoselov, K.S.; Qiu, C.-W. Geometric filterless photodetectors for mid-infrared spin light. Nat. Photonics **2023**, 17, 171–178. [CrossRef]

311. Xie, J.; Ren, Z.; Wei, J.; Liu, W.; Zhou, J.; Lee, C. Zero-Bias Long-Wave Infrared Nanoantenna-Mediated Graphene Photodetector for Polarimetric and Spectroscopic Sensing. Adv. Opt. Mater. **2023**, 11, 2202867. [CrossRef]

312. Dai, M.;Wang, C.; Ye, M.; Zhu, S.; Han, S.; Sun, F.; Chen,W.; Jin, Y.; Chua, Y.;Wang, Q.J. High-Performance, Polarization-Sensitive, Long-Wave Infrared Photodetection via Photothermoelectric Effect with Asymmetric van der Waals Contacts. ACS Nano **2022**, 16, 295–305. [CrossRef]

313. Xu, S.; Ren, Z.; Dong, B.; Zhou, J.; Liu,W.; Lee, C. Mid-Infrared Silicon-on-Lithium-Niobate Electro-Optic Modulators Toward Integrated Spectroscopic Sensing Systems. Adv. Opt. Mater. **2022**, 11, 2202228. [CrossRef]

314. Ma, Y.; Chang, Y.; Dong, B.; Wei, J.; Liu, W.; Lee, C. Heterogeneously Integrated Graphene/Silicon/Halide Waveguide Photodetectors toward Chip-Scale Zero-Bias Long-Wave Infrared Spectroscopic Sensing. ACS Nano **2021**, 15, 10084–10094. [CrossRef]